EPR Spectroscopy on Mononuclear Molybdenum-Containing Enzymes

Luisa B. Maia, Isabel Moura, and José J.G. Moura

Abstract The biological relevance of molybdenum was demonstrated in the early 1950s-1960s, by Bray, Beinert, Lowe, Massey, Palmer, Ehrenberg, Pettersson, Vänngård, Hanson and others, with ground-breaking studies performed, precisely, by electron paramagnetic resonance (EPR) spectroscopy. Those earlier studies, aimed to investigate the mammalian xanthine oxidase and avian sulfite oxidase enzymes, demonstrated the surprising biological reduction of molybdenum to the paramagnetic Mo^{5+}. Since then, EPR spectroscopy, alongside with other spectroscopic methods and X-ray crystallography, has contributed to our present detailed knowledge about the active site structures, catalytic mechanisms and structure/activity relationships of the molybdenum-containing enzymes.

This Chapter will provide a perspective on the contribution that EPR spectroscopy has made to some selected systems. After a brief overview on molybdoenzymes, the Chapter will be focused on the EPR studies of mammalian xanthine oxidase, with a brief account on the prokaryotic aldehyde oxidoreductase, nicotinate dehydrogenase and carbon monoxide dehydrogenase, vertebrate sulfite oxidase, and prokaryotic formate dehydrogenases and nitrate reductases.

Keywords EPR • Magnetic interactions • Molybdenum • Enzymes • Xanthine oxidase/xanthine dehydrogenase • Aldehyde oxidase • Aldehyde oxidoreductase • Nicotinate dehydrogenase • Carbon monoxide dehydrogenase • Sulfite oxidase • Nitrate reductases • Formate dehydrogenases • Dimethylsulfoxide reductas

Abbreviations

AO	Mammalian aldehyde oxidase
AOR	Bacterial molybdenum-containing aldehyde oxidoreductases
CW EPR	Continuous wave electron paramagnetic resonance spectroscopy

L.B. Maia (✉) • I. Moura • J.J.G. Moura (✉)
UCIBIO, REQUIMTE, Departamento de Química, Faculdade de Ciências e Tecnologia, Universidade Nova de Lisboa, 2829-516 Caparica, Portugal
e-mail: luisa.maia@fct.unl.pt; isabelmoura@fct.unl.pt; jose.moura@fct.unl.pt

G. Hanson, L. Berliner (eds.), *Future Directions in Metalloprotein and Metalloenzyme Research*, Biological Magnetic Resonance 33,
DOI 10.1007/978-3-319-59100-1_4

DMS	Dimethylsulfide
DMSO	Dimethylsulfoxide
DMSOR	Dimethylsulfoxide reductase
ENDOR	Electron nuclear double resonance spectroscopy
EPR	Electron paramagnetic resonance spectroscopy
FDH	Formate dehydrogenase (all types of formate dehydrogenase enzymes)
FDH-H	*E. coli* formate dehydrogenase H, from the formate-hydrogen lyase system
FDH-N	*E. coli* formate dehydrogenase N, from the anaerobic nitrate-formate respiratory pathway
Fe/S	Iron-sulfur centre
FYX (FYX-051)	4-[5-pyridin-4-yl-1H-[1,2,4]triazol-3-yl]pyridine-2-carbonitrile
mARC	Mitochondrial amidoxime reducing component
MOSC	From molybdenum cofactor sulfurase C-terminal domain (proteins involved in pyranopterin cofactor biosynthesis)
NaR	Nitrate reductase (all types of nitrate reductase enzymes, prokaryotic and eukaryotic ones)
NaRGHI	Respiratory nitrate reductase (prokaryotic), after the name of the encoding genes, *narG*, *H*, and *I*
NaRZWV	Respiratory nitrate reductase (prokaryotic), after the name of the encoding genes, *narZ*, *W*, and *V*
SO	Sulfite oxidase
XAS	X-ray absorption spectroscopy
XO	Xanthine oxidase

Introduction

The biological relevance of molybdenum was demonstrated in the early 1950s–1960s, by Bray, Beinert, Lowe, Massey, Palmer, Ehrenberg, Pettersson, Vänngård, Hanson and others, with ground-breaking studies performed, precisely, by *electron paramagnetic resonance* (*EPR*) *spectroscopy*. Those earlier studies, aimed to investigate the mammalian xanthine oxidase and avian sulfite oxidase enzymes, demonstrated the surprisingly biological reduction of molybdenum to the paramagnetic Mo^{5+}. Since then, EPR spectroscopy, alongside with other spectroscopic methods and X-ray crystallography, has contributed to our present detailed knowledge about the active site structures, catalytic mechanisms and structure/activity relationships of the molybdenum-containing enzymes. The great majority of the studies have employed continuous wave (CW) EPR, but advanced EPR-related methods were also decisive.

Molybdenum, $_{42}$Mo, is a transition metal element, belonging to the sixth group of the "d-block" of the Periodic Table, with electronic configurations [Kr] $4d^5\ 5s^1$. The paramagnetic Mo^{5+}, [Kr] $4d^1$, formed during the normal enzyme catalytic cycle

or produced artificially, gives rise to characteristic d^1, $S = 1/2$, signals, with $\Delta g < 0.4$ [1]. Although the three values of g were expected to be lower than two, this is frequently not the case, as will be described (Table 1). In addition, the hyperfine structure arising from the molybdenum nucleus itself ($I = 5/2$, from ^{95}Mo and ^{97}Mo, naturally present in ca 16 and 9%, respectively) can be observed.

The relatively narrow lines of Mo^{5+} signals (small linewidths) allow the observation of weak hyperfine interactions with atoms in the close proximity of the molybdenum atom (although the IUPAC recommended denomination for this interaction type is "superhyperfine interaction", in opposition to the parent nucleus hyperfine interaction, herein, for simplicity, "hyperfine" will be used). This feature has been explored to probe the structure of the molybdenum first and second coordination spheres, in most cases using enzymes and/or substrates/inhibitors labelled with ^{2}H ($I = 1$), ^{13}C ($I = 1/2$), ^{15}N ($I = 1/2$), ^{17}O ($I = 5/2$), ^{33}S ($I = 3/2$) and others.

Given the large number of molybdoenzymes, this chapter does not intended to be exhaustive. Instead, to restrict the information presented to a manageable size, this Chapter will provide only a perspective on the contribution that EPR spectroscopy has made to some selected systems. Hence, after a brief overview on molybdoenzymes (section "An Overview on Molybdenum-Containing Enzymes"), the Chapter will be focused on the EPR studies of mammalian xanthine oxidase, with a brief account on the prokaryotic aldehyde oxidoreductase, nicotinate dehydrogenase and carbon monoxide dehydrogenase (section "Xanthine Oxidase Family"), vertebrate sulfite oxidase (section "Sulfite Oxidase Family"), and prokaryotic formate dehydrogenases and nitrate reductases (section "Dimethylsulfoxide Reductase Family") (Table 1).

An Overview on Molybdenum-Containing Enzymes

Molybdenum is essential to most organisms [2, 3], from archaea and bacteria to higher plants and mammals [4–11]. Actually, it is relevant for all life on Earth. Molybdenum is central to the nitrogen biogeochemical cycle, where it is mandatory for the atmospheric dinitrogen fixation (reduction) into ammonium (nitrogenase). The recent "nitrogen-to-molybdenum bio-to-inorganic bridge hypothesis" defend that the molybdenum scarcity in the Early Earth (ca 1800 Myr ago) could have delayed the evolutionary path of eukaryotes for ca 2000 Myr, by limiting the rate of dinitrogen fixation and, thus, the availability of fixed nitrogen for the early organisms [11–17]. In addition, the nitrate reduction to nitrite (nitrate reductases) and nitrite oxidation to nitrate (nitrite oxidoreductases) also depend on this metal. Molybdenum has also been suggested to be involved in the nitrite reduction to nitric oxide for signalling and survival of mammalian cells under challenging conditions [18–23]. Molybdenum is also involved in the carbon cycle, where it is used to fix (reduced) carbon dioxide into formate (formate dehydrogenases [24–26]) or interconvert aldehydes and carboxylic acids, produce plant hormones or participate in the mammalian xenobiotic metabolism (plant [27–29] and mammalian aldehyde oxidases [30–37]) or in the purine catabolism (xanthine hydroxylation to urate by

Table 1 Representative X-band EPR signals form mononuclear molybdenum-containing enzymes

Signal	$g_{1,2,3}$	$A_{1,2,3}$ (H) (MHz)[a]
Xanthine oxidase family		
Xanthine oxidase		
"Very rapid"	2.025, 1.955, 1.949	–
"Alloxanthine"	2.028, 1.959, 1.944	–
"Rapid type 1"	1.989, 1.969, 1.965	36.2, 38.3, 38.5 11.1, 8.3, 5.5
"Rapid type 2"	1.989, 1.969, 1.965	39.0, 42.0, 45.3 27.9, 29.4, 37.5
"Slow"	1.972, 1.967, 1.955	44.7, 44.4, 42.6 3.9, 4.5, 6.3
"Inhibited"	1.991, 1.977, 1.951	12.3, 10.8, 15.3
"Desulfo-inhibited"	1.980, 1.973, 1.967	–
"Arsenite"	1.973, 1.972, 1.926	–
"Mercurial"	1.969, 1.958, 1.943	–
Desulfovibrio gigas aldehyde oxidoreductas		
"Rapid type 2"	1.988, 1.970, 1.964	32.0, 45.8, 34.6 31.7, 17.4, 25.6
"Slow"	1.971, 1968, 1.958	46.4, 44.1, 39.5
"Arsenite"	1.979, 1.972, 1.922	–
Eubacterium barkeri nicotinate dehydrogenase		
"Very rapid" like	2.067, 1.982, 1.974	–
Oligotropha carboxidovorans carbon monoxide dehydrogenase		
"Mo/Cu"	2.001, 1.960, 1.955	–[b]
Sulfite oxidase family		
Sulfite oxidase		
"Low pH"	2.004, 1.972, 1.966	23.8, 22.1, 35.8 4, 6, 4
"High pH"	1.987, 1.964, 1.953	–[c]
"Phosphate-inhibited"	1.992, 1.969, 1.974	–
Dimethylsulfoxide reductase family		
Formate dehydrogenases		
Escherichia coli formate dehydrogenase H	2.094, 2.001, 1.990	7.5, 18.9, 20.9
Desulfovibrio desulfuricans formate dehydrogenase	2.012, 1.996, 1.985	23.1, 29.9, 27.8 35.1, nd, nd
Ralstonia eutropha NAD-dependent formate dehydrogenase	2.009, 2.001, 1.992	18, 21, 18
D. alaskensis molybdenum-containg formate dehydrogenase	1.971, 1.968, 1.959	44.2, 44.1, 43.9
Periplasmatic nitrate reductase		
Paracoccus pantothrophus periplasmatic nitrate reductase		
"Low *g*-unsplit"	1.997, 1.962, 1.959	–
"Low *g*-split"	1.996, 1.969, 1.961	36.3, 37.5, 42.0
"Very high *g*"	2.022, 1.999, 1.994	20.9, 20.7, 18.4

(continued)

Table 1 (continued)

Signal	$g_{1,2,3}$	$A_{1,2,3}$ (H) (MHz)[a]
"High *g*"	1.999, 1.990, 1.981	17.9, 14.5, 13.9 8.4, nd, nd
"High *g*-nitrate"	1.999, 1.989, 1.982	17.9, 12.0, 12.8 9.0, nd, nd
Desulfovibrio desulfuricans periplasmatic nitrate reductase		
"High *g*-nitrate"	2.000, 1.990, 1.981	12.9, 13.9, 12.8
"High *g*-turnover"	1.999, 1.992, 1.982	16.2, 18.1, 15.3 16.2, 18.1, 15.3
Assimilatory nitrate reductase		
Synechococcus sp. PCC 7942 assimilatory nitrate reductase		
"Very high *g*"	2.023, 1.998, 1.993	–
"high *g*"	1.997, 1.990, 1.982	–
Respiratory nitrate reductases		
Escherichia coli respiratory nitrate reductase		
"Low pH"	2.001, 1.986, 1.964	31.7, 23.6, 24.7
"High pH"	1.988, 1.981, 1.962	10.6, 8.9, 9.1
Paracoccus pantothrophus respiratory nitrate reductase		
"Low pH"	2.007, 1.987, 1.970	nd
"High pH"	1.990, 1.989, 1.967	nd
M. hydrocarbonoclasticus respiratory nitrate reductase		
"Low pH-nitrate"	1.996, 1.982, 1979	nd
"High pH-nitrtate"	2.002, 1.987, 1968	39.2, 30.6, 30.3

[a]*nd* not detected
[b]$A_{1,2,3}$(Cu) = 117, 164, 132 MHz
[c]An ENDOR study demonstrated the presence of a solvent-exchangeable, strongly and anisotropically coupled proton in this signal [253–255]

xanthine oxidoreductase [38–44]). The role of molybdenum is also extended to the sulfur cycle, where it is used in the respiratory oxidation of inorganic sulfur compounds (sulfite-oxidising enzymes) [45–48]. It is also critical to the catabolism of sulfur-containing compounds, being vital for human cells that must eliminate (oxidise) the toxic sulfite to survive (sulfite oxidase) [49–54].

Presently, more than 50 molybdenum-containing enzymes are known, many of which have been biochemically and structurally characterised, and the number is increasing every year, with several more being foreseen to be "discovered" in a near future based on genomic analyses. Noteworthy, the great majority of the molybdoenzymes are prokaryotic, whereas only a restricted number of molybdoenzymes are found in eukaryotes.

Organisms use molybdenum in the active site of enzymes that catalyse (almost exclusively) oxidation/reduction reactions at carbon, nitrogen and sulfur atoms of key metabolites, most of which involve the transfer of one oxygen atom [4–11]. The chemical properties of molybdenum are perfectly suitable for this "Redox

Biochemistry" [55]: it is redox-active under physiological conditions, where its oxidation state can range from 6+, 5+ and 4+, and even 3+, in nitrogenase [56, 57]; it can have a very versatile first coordination sphere; its chemistry is dominated by the formation of oxides and sulfides, where its strong tendency to bind oxo groups is balanced by its ability to easily lose a single oxygen atom. This feature makes molybdenum centres excellent "oxygen atom exchangers" [58–66], as long as the thermodynamics of the reaction of "oxygen exchange" is favourable (Eqs. (1) and (2)) [59, 64, 67], what has led to the "oxo transfer hypothesis" coined by Holm and others in the 1980s. Organisms explore this rich chemistry to carry out different oxotransfer reactions (see Eqs. (5), (6), (7), (8), (9), (10), and (11) in section "EPR Studies of Molybdoenzymes"), where one oxygen atom is transferred from water to product -*oxygen atom insertion* (Eq. (3))- or from substrate to water -*oxygen atom abstraction* (Eq. (4)). These reactions involve a net exchange of two electrons, with the molybdenum atom cycling between Mo^{6+} and Mo^{4+} (Eqs. (3) and (4)), and, most importantly, with the metal being the direct oxygen atom donor or acceptor (Eqs. (1) and (2)) [4–11, 31, 35, 38, 41, 42, 44]. Subsequently, the initial metal oxidation state is regenerated, in most of the cases, by two one-electron oxidation/reduction reactions ($Mo^{6+} \leftrightarrow Mo^{5+} \leftrightarrow Mo^{4+}$) with other redox-active cofactors within the enzyme (iron-sulfur (Fe/S) centres, haems, flavins). Noteworthy, some molybdoenzymes are able to catalyse both oxygen atom insertion and abstraction during the same catalytic cycle [11, 18–23, 68].

$$\mathrm{Mo-O+X \rightarrow Mo+X-O} \tag{1}$$

$$\mathrm{Mo+X-O \rightarrow Mo-O+X} \tag{2}$$

$$\mathrm{Mo^{6+}+Q+H_2O \rightarrow Mo^{4+}+Q-O+2H^{+}} \tag{3}$$

$$\mathrm{Mo^{4+}+R-O+2H^{+} \rightarrow Mo^{6+}+R+H_2O} \tag{4}$$

The versatile chemistry of molybdenum allows it to also catalyse reactions of sulfur atom transfer [69–73], hydrogen atom transfer (Eq. (12), in section "EPR Studies of Molybdoenzymes") and even a non-redox hydration reaction (the acetylene hydratase-catalysed hydration of acetylene to acetaldehyde).

Structurally, molybdenum is found in the enzymes active site in a mononuclear form [4–11], except in nitrogenase, where it is present in the unique heteronuclear [$MoFe_7S_9C$], and in a few other cases[1]. In the mononuclear molybdenum centres, one molybdenum atom is coordinated by the *cis*-dithiolene (–S–C=C–S–) group of one or two pyranopterin cofactor molecules (Fig. 1a) and by oxygen and/or sulfur and/or selenium atoms in a diversity of arrangements. Based on the *metal center structure*,

[1] The carbon monoxide dehydrogenase from *Oligotropha carboxidovorans* or *Hydrogenophaga pseudoflava*, with its unique binuclear Mo/Cu cofactor (Mo-S-Cu-S(Cys)) [74–78], as well as a few other heteronuclear centres of proteins whose physiological function is not yet fully understood [79–84], are exceptions to the mononuclear presence of molybdenum. In spite of that, the carbon monoxide dehydrogenase is classified as a member of the xanthine oxidase family.

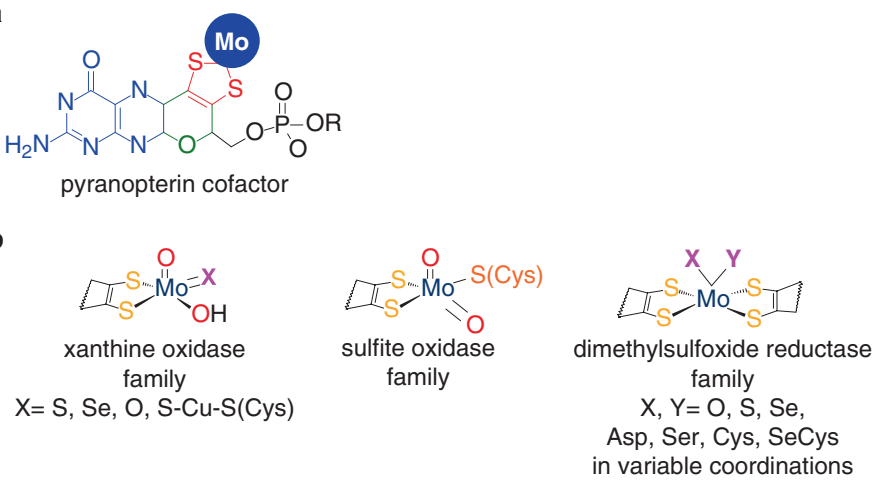

Fig. 1 Structures of the pyranopterin cofactor (**a**) and of the active site of molybdenum-containing enzymes. (**a**) The pyranopterin cofactor molecule is formed by pyrano(*green*)-pterin(*blue*)-dithiolene(*red*)-methylphosphate(*black*) moieties. The dithiolene (–S–C=C–S–) group forms a five-membered ene-1,2-dithiolate chelate ring with the molybdenum/tungsten atom. In eukaryotes, the cofactor is found in the simplest monophosphate form (R is a hydrogen atom), while in prokaryotes it is most often found esterified with several nucleotides (R can be one cytidine monophosphate, guanosine monophosphate or adenosine monophosphate). (**b**) Structures of the molybdenum centres of the three families of molybdoenzymes in the oxidised form. For simplicity, only the *cis*-dithiolene group of the pyranopterin cofactor is represented. Adapted with permission from [21]

the mononuclear molybdoenzymes are organised into three families, denominated after one benchmark enzyme (Fig. 1b) [4], which will be described in the following sections: xanthine oxidase (XO; section "Xanthine Oxidase Family") family, sulfite oxidase (SO; section "Sulfite Oxidase Family") family and dimethylsulfoxide reductase (DMSOR; section "Dimethylsulfoxide Reductase Family") family.

EPR Studies of Molybdoenzymes

Xanthine Oxidase Family

The Enzymes

The active site of the XO family enzymes (in its oxidised form; Fig. 1b) has a molybdenum atom coordinated in a distorted square-pyramidal geometry by an apical oxo group (Mo=O) and, in the equatorial plane, by the two sulfur atoms of the *cis*-dithiolene group of one pyranopterin cofactor molecule, one catalytically labile -OH group (in almost all enzymes) plus one terminal sulfo (Mo=S; in most

enzymes) or seleno (Mo=Se) or oxo (Mo=O) or Mo-S-Cu-S(Cys) moiety (see note 1) [4–11, 31, 35]. This family comprises the prototype mammalian (bovine milk) XO (Eq. (5)) and other enzymes such as mammalian aldehyde oxidases (AO), *Desulfovibrio* aldehyde oxidoreductases (AOR), *Eubacterium barkeri* nicotinate dehydrogenase, *Oligotropha carboxidovorans* carbon monoxide dehydrogenase, *Pseudomonas putida* quinoline 2-oxidoreductase or *Thauera aromatica* 4-hydroxybenzoyl-CoA reductase.

Structurally, mammalian XO is an homodimeric enzyme, with each monomer holding two [2Fe-2S] centres and one FAD, besides one molybdenum centre [38, 41, 42, 44, 85, 86]. The four redox-active centres are aligned in an almost linear fashion, defining an intramolecular electron transfer pathway that delivers electrons from the molybdenum centre to the FAD, the sites where the hydroxylation (Eq. (6)) and dioxygen reduction (Eq. (7)) take place, respectively, with Fe/S centres intermediating the electron transfer between the two.

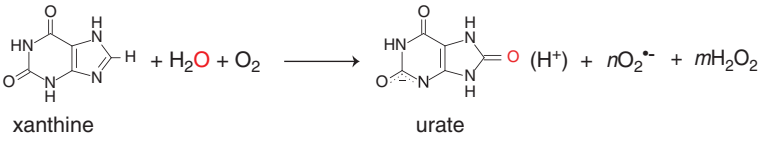

(5)

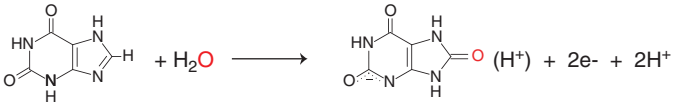

(6)

$$O_2 + 2e^- + 2H^+ \rightarrow nO_2^{\cdot -} + mH_2O_2 \quad (7)$$

XO family enzymes typically catalyse the hydroxylation of a C–H moiety in aromatic heterocyclic compounds and aldehydes [31, 35, 38, 41, 42, 44]. For this, the enzymes molybdenum centre has to promote the cleavage of a C–H bond and the formation of a novel C–O bond, as the XO-catalysed reaction of xanthine hydroxylation to urate illustrates (Eq. (6)). The molecular mechanism of XO-catalysed hydroxylation reaction is presently well established and believed to be essentially similar in other members of this family, namely in AO and AOR enzymes (Fig. 2) [31, 35, 38, 41, 42, 44, 85–89]: (1) the catalysis is initiated with the activation of the molybdenum catalytically labile hydroxyl group (Mo-OH) by a neighbouring conserved deprotonated glutamate residue, to form an Mo^{6+}-O^- core (base-assisted catalysis); (2) the now deprotonated oxygen undertakes nucleophilic attack on the carbon atom to be hydroxylated, with the simultaneous transfer of hydride from substrate to the essential sulfo group (Mo=S → Mo–SH), resulting in the formation of a covalent intermediate, Mo^{4+}-O-C-R(-SH) (where R represents the remainder of the substrate molecule); (3) hydroxide/water (from solvent) then displaces the hydroxylated product from the molybdenum coordination sphere to yield a Mo^{4+}-$OH_{(2)}$(-SH) core (oxidation half-reaction; Eq. (6)); (4) the two electrons transferred from the substrate to the molybdenum (Mo^{6+} → Mo^{4+}) during the

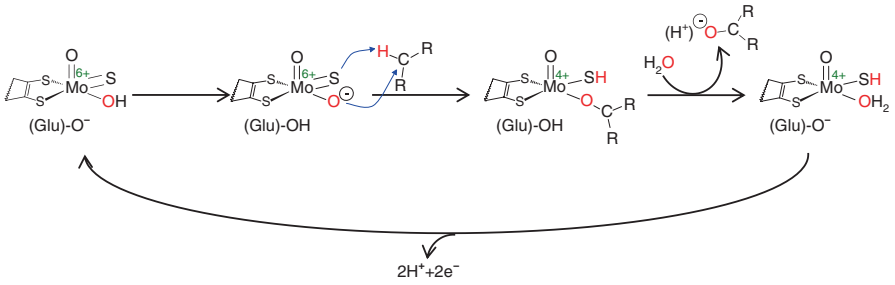

Fig. 2 Mechanism of xanthine oxidase-catalysed hydroxylation reaction. See text for details

oxidative half-reaction are rapidly transferred, via the Fe/S centres, to the FAD (Mo → Fe/S → FAD), where the reduction of dioxygen takes place (reductive half-reaction; Eq. (7)); (5) in the now oxidised molybdenum centre ($Mo^{4+} \rightarrow Mo^{6+}$), the sulfo group is deprotonated and the initial Mo^{6+}-OH(=S) core is regenerated.

The critical role of the terminal sulfo group, Mo=S (Fig. 2), in catalysis is revealed when, after its removal, the enzymes hydroxylation activity is completely abolished [90, 91]. The chemical removal of the sulfo group is achieved through reaction with cyanide, which abstracts the sulfur atom in the form of thiocyanide and leaves an oxo group, Mo=O, in its place. The modified enzyme form is denominated "desulfo", in opposition to the "sulfo" form of native enzyme. Noteworthy, the desulfo form can be converted into the sulfo form (Mo=O → Mo=S) by sulfuration through reaction with sulfide (Na_2S). "Desulfo" XO molecules occur naturally in cells and are the result of inefficient in vivo sulfuration [92–94].

Two other features of the XO reaction mechanism have to be here highlighted. First, water is the ultimate source of the oxygen atom incorporated into the hydroxylated product (Eq. (6); Fig. 2), as is characteristic of molybdoenzymes, with dioxygen being *only* the oxidising substrate [95–97] (Eq. (7)). The direct oxygen donor is the catalytically labile equatorial Mo-OH group of the molybdenum center; this group (this oxygen atom) is subsequently regenerated by a water molecule from the solvent, in the end of each catalytic cycle. Second, the hydroxylation reaction occurs through one two-electron reduction of the molybdenum centre ($Mo^{6+} \rightarrow Mo^{4+}$) [98] and the intramolecular electron transfer to other redox centres within the enzyme (Mo → Fe/S → FAD, in the case of XO) is an integral aspect of the catalysis. Hence, the Mo^{5+} species observed by EPR spectroscopy related to hydroxylation reactions are formed through the oxidation of the Mo^{4+} species.

EPR Studies of Mammalian Xanthine Oxidase

Being one of the most studied molybdoenzymes, our present knowledge about XO structure and reaction mechanism, together with the information gathered from the study of model compounds [66, 99–102], allows us to discuss its EPR signals in

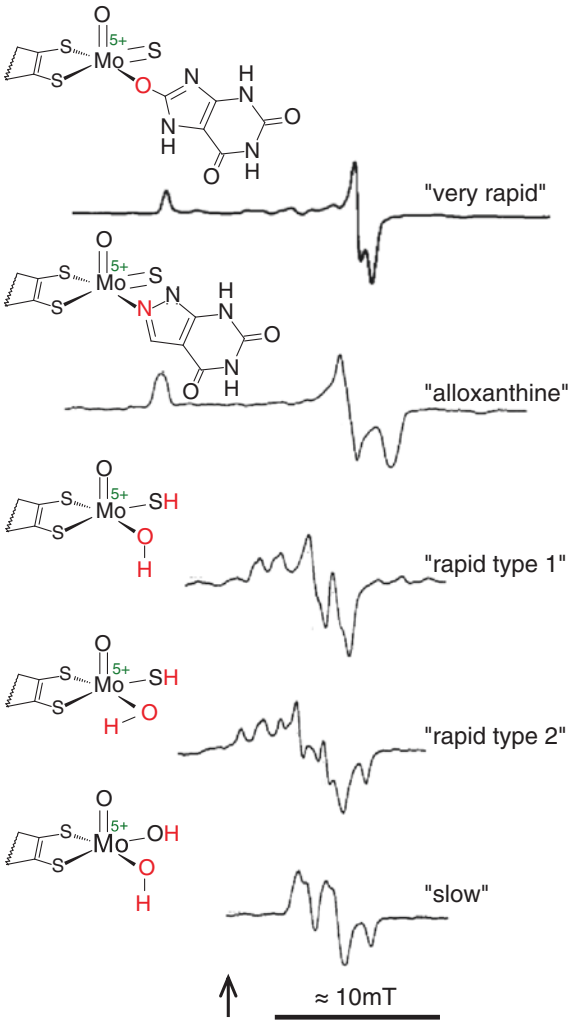

Fig. 3 Representative X-band EPR spectra of xanthine oxidase Mo^{5+} "very rapid", "alloxanthine", "rapid type 1", "rapid type 2" and "slow" signals and the respective structures proposed for each signal-giving species. "Very rapid" signal obtained with xanthine; adapted with permission from [104], copyright (1988) American Chemical Society. "Alloxanthine" signal; adapted with permission from [112]. "Rapid type 1" signal obtained with purine; adapted with permission from [145], copyright (1982) American Chemical Society. "Rapid type 2" signal obtained with dithionite in the presence of borate; adapted with permission from [145], copyright (1982) American Chemical Society. "Slow" signal obtained with dithionite; adapted with permission from [145], copyright (1982) American Chemical Society. The *arrow* indicates the position of $g = 2.0037$

detail and to draw a clear picture of the structure of each signal-giving species—as will be discussed in the following sections (Figs. 3 and 4).

The biological relevance of molybdenum was unambiguously and definitively demonstrated by Bray and Meriwether in 1966 [103] using XO purified form milk of cows that had been injected with ^{95}Mo-labelled molybdate (e.g., $A_{1,2,3}(^{95}\text{Mo})$ = 133, 54.7, 57.3 MHz, with xanthine, in the "very rapid" signal [104]). Those earlier studies demonstrated the surprising presence and catalytic role of molybdenum in a mammal [105, 106].

The XO Mo^{5+} can give rise to different EPR signals, depending on the enzyme form ("sulfo", "desulfo", inhibited), the compound used to reduce the enzyme (purine derivates, aldehydes, artificial reductants, etc) and on the time of reduction.

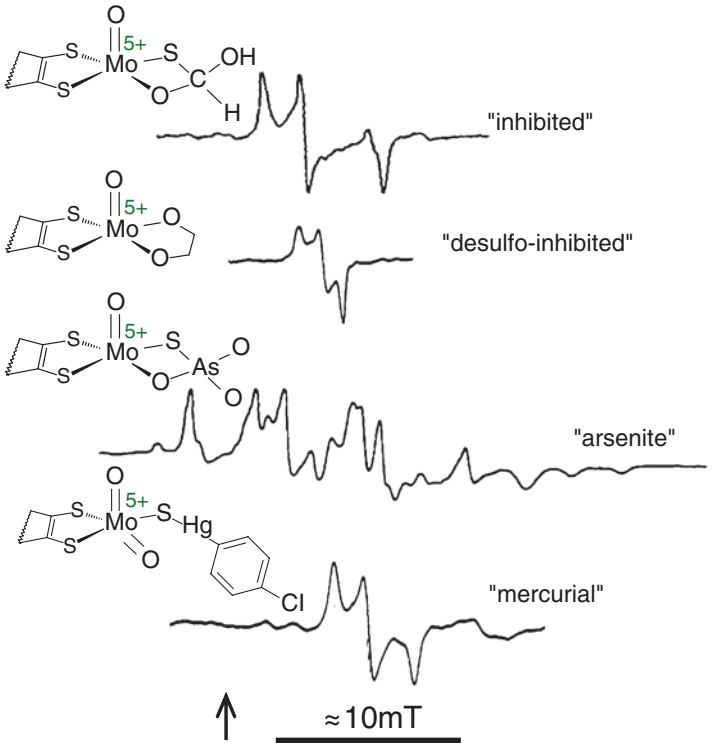

Fig. 4 Representative X-band EPR spectra of xanthine oxidase Mo^{5+} "inhibited", "desulfo-inhibited", "arsenite" and "mercurial" signals and the respective structures proposed for each signal-giving species. "Inhibited" signal obtained with formaldehyde; adapted with permission from [158]. "Desulfo-inhibited" signal obtained with ethylene-glycol; adapted with permission from [145], copyright (1982) American Chemical Society. "Arsenite" signal obtained with arsenite-treated and dithionite-reduced enzyme; adapted with permission from [165]; copyright (1983) American Chemical Society. "Mercurial" signal obtained with *p*-chloro-mercuri-benzoate; adapted with permission from [168]; copyright (1983) American Chemical Society. The *arrow* indicates the position of $g = 2.0037$

The signals were originally named by Bray and Vänngård [107], based on the relative rate of their formation and decay in the course of the reaction of enzyme with substrate, as "very rapid" ($t_{1/2} \approx 10^{-2}$ s), "rapid" ($t_{1/2} \approx 10^{-1}$ s), "slow" ($t_{1/2} \approx 10^{3}$ s) and "inhibited" ($t_{1/2} \approx 10^{6}$ s) signals (Figs. 3 and 4). Later, the observation of other signals led to the introduction of the "desulfo-inhibited", "arsenite" or "mercurial" signals.

The "Very Rapid" Signal

The "very rapid", originated from XO molecules in the native, sulfo, form, is a nearly axial signal ($g_1 \gg g_2 \approx g_3$), with $g_1 > 2$ ($g_{1,2,3} = 2.025, 1.955, 1.949$, with xanthine [108]), that does not display hyperfine structure due to coupled protons

(Fig. 3) [108, 109]. This signal was observed for the first time in 1964, by Palmer et al. [105], in the presence of an excess of xanthine, after a short reaction period (8 ms). Subsequent studies showed that the signal could also be obtained in the presence of sub-stoichiometric amounts of xanthine (either anaerobically or aerobically), as well as, with hypoxanthine, 1-methyl-xanthine, 6-methyl-purine, 2-hydroxy-6-methyl-purine, 8-hydroxy-6-methyl-purine or 2,4-dihydroxypteridine, being its formation favoured by high pH values [106, 109–112]. The species that gives rise to the "very rapid" signal is thought for long to be a catalytic intermediate, formed by oxidation of a Mo^{4+}-substrate complex [107, 109, 113].

Studies with ^{13}C8-labelled xantina (the position that is hydroxylated by the enzyme), in ^{17}O-labelled water (the oxygen that is ultimately incorporated in urate), resulted in a "very rapid" signal splitted approximately isotropically by both nuclei ($A_{1,2,3}(^{13}C)$ = 11.1, 7.6, 7.6 MHz [108] and $A_{1,2,3}(^{17}O)$ = 38.0, 38.3, 37.1 MHz [104, 108, 109, 114, 115]). The strong isotropic hyperfine coupling to ^{17}O was taken as the main evidence for the presence of a Mo-$O_{non\text{-}terminal}$ bond (Mo-O-R) in the signal-giving species (in opposition to the small and quite anisotropic interaction ($A_{1,2,3}(^{17}O)$ = 8.6, 8.6, 1.9 MHz) observed in model compounds with a terminal oxo group, Mo=O [116]). In its turn, the splitting induced by ^{13}C showed that the xanthine C8 is located within magnetic contact to the molybdenum atom and, although the small interaction value could arise from an equatorial Mo-C8(xanthine) complex (that is, from an equatorial ligand σ-bonded to the molybdenum, with the ligand laying on a node of the ground-state orbital), that hypothesis is difficult to rationalise mechanistically and to reconcile with the above Mo-O-R interpretation. Hence, the signal was interpreted as probably arising form of a Mo^{5+}-O-C8(xanthine) complex.

Noteworthy, alloxanthine originates an EPR Mo^{5+} signal very similar to the "very rapid", also nearly axial, with $g_1 > 2$ (2.028, 1.959 and 1.944) and with no coupled protons (Fig. 3) [112, 114]. Alloxanthine, a xanthine isomer that holds one nitrogen atom (N2) in place of the xanthine C8, is a powerful inhibitor of the hydroxylation activity of XO [117]. In the presence of alloxanthine, the XO Mo^{5+} interacts isotropically with a single nitrogen atom (presumably the alloxanthine N2; $a_{1,2,3}(^{14}N)$=9.9, 9.6, 8.7 MHz), but not with ^{17}O, probably through a Mo^{5+}-N2(alloxanthine) complex [112].

The use of ^{95}Mo- and ^{97}Mo-enriched XO (^{95}Mo, I = 5/2, no significant nuclear electric quadrupole; ^{97}Mo, I = 5/2, strong nuclear electric quadrupole) showed a strong anisotropic hyperfine coupling, as well as, nuclear electric quadrupole interaction, with $A_{1,2,3}(^{95}Mo)$ = 142, 60.1, 63.4 MHz, with non-coincident $\boldsymbol{g}$ and $\boldsymbol{A}$ tensors axes (with Euler angles of $\alpha = 7°$, $\beta = 42°$ and $\gamma = 0°$) and $P_{1,2,3}(^{97}Mo)$ = 4.0, −5.5, 1.5 MHz, with coincident $\boldsymbol{P}$ and $\boldsymbol{A}$ tensors axes (using 2-hydroxy-6-methyl-purine) [104]. The highly anisotropic $\boldsymbol{P}$, with the largest principal axis pointing along A_2, was most consistent with a MoOS structure for the "very rapid" signal-giving species. Using density functional theory, Drew and Hanson [118] and others [119, 120] suggested that the non-coincidence angle β could provide a measure of the metal-dithiolene fold angle of the molybdenum centre (defined by the dihedral angle between the MoS_2 plane and the S_2C_2 plane of the pyranopterin molecule). Accordingly, the above mentioned angle β of 42° would correspond to a metal-dithiolene fold angle of 15° [118]. Although this value is somewhat different from

the 21° observed in the crystal structure of XO complexed with 2-hydroxy-6-methyl-purine [87] or with FYX [86], it can be argued that crystallographic structures represent a weighted mean of oxidation states (Mo^{6+}, Mo^{5+}, Mo^{4+}).

When the "very rapid" signal is generated from XO molecules that were desulfurated (reaction with cyanide) and resulfurated with ^{33}S-labelled sulfide (reaction with $Na_2{}^{33}S$), a strong and anisotropic interaction is observed ($A_{1,2,3}(^{33}S)$ = 8.5, 76.6, 19.1 MHz, with xanthine) [91, 104, 121, 122]. The related signal originated in the presence of alloxanthine also displays a similar coupling to ^{33}S ($A_{1,2,3}(^{33}S)$ = 8.5, 85.0, 19.1 MHz) [112, 123]. The observed anisotropy suggested that the sulfur atom would be a terminal ligand, Mo=S and not Mo-S-R (contrary to the oxygen atom, that would be as Mo-O-R and not Mo=O); the absence of hyperfine coupling to protons depicted this sulfur as a Mo=S (and not Mo-S-H). Furthermore, because the equatorial ligands originate stronger interactions than the axial ligands in model compounds, the sulfur atom was suggested to be in an equatorial position [122, 124]. The magnitude of the $Mo^{5+}/^{33}S$ anisotropic interaction, unexpected for an isotope with a small nuclear g value (g_n of 0.429), suggests that the sulfur p orbital participates to a large extent in the ground-state molecular orbital of the signal-giving species, with the unpaired electron delocalised ca 38% over the sulfur [104, 109, 122] (calculated based on the expected anisotropic coupling of 156 MHz, if the unpaired electron resided entirely in a sulfur p orbital [125]). Also the unusually high value of g_1 (that makes the signal look like an axial one) was suggested to result mainly from spin-orbit coupling with filled orbitals involving this sulfur, supporting the claim that a $g > 2$ is evidence for sulfur ligation [104]. If the unpaired electron is delocalised over the sulfur, then one group exerting a strong ligand field is necessary to bring the ground-state orbital into approximately the same plane as the sulfo group [104]. In 1985, Bray and George [109] (without having any evidence for its existence, now confirmed by X-ray crystal structures) ingeniously suggested the presence of one "spectator" axial oxo group.

In summary, the structure of "very rapid" signal-giving species suggested by the EPR data is a **$Mo^{5+}(=O_{axial})(=S_{equatorial})$-$O_{equatorial}$-C(xanthine)** complex (Fig. 3). This structure was entirely confirmed, when the crystallographic structure of oxidised XO [85] and of the key intermediate in the hydroxylation reaction of FYX by XO [86] were solved. The reduced enzyme-substrate (XO-FYX) complex obtained by Okamoto et al. [86] revealed the presence of an axial oxo group and one equatorial sulfo group, unambiguously modelled as a Mo-SH, as well as the substrate molecule bound through the labile oxygen atom to the molybdenum atom. This reduced enzyme-substrate complex, in which the carbon–oxygen bond of the product was already formed, but the product remained bound to the molybdenum, can, thus, be formulated as a $Mo^{4+}(=O_{axial})(-SH_{equatorial})$-$O_{equatorial}$-C(FYX) complex. The following cleavage of the Mo^{4+}-O bond results in the hydroxylated product release; the $Mo^{4+}(=O_{axial})(-SH_{equatorial})$-$OH_{equatorial}$ complex formed is subsequently oxidised, via intramolecular electron transfer, to regenerate the initial Mo^{6+} complex. The Mo^{4+}-substrate reaction intermediate can, however, follow an alternative pathway, in which it is first one-electron oxidised to the Mo^{5+}-substrate species that gives rise to the "very rapid" signal and, only then, cleaved to release the hydroxylated product.

Accordingly, it is the balance between the rate of Mo^{4+}-substrate oxidation to Mo^{5+}-substrate and the rate of product release from Mo^{4+}-substrate that determines if a given substrate can, or not, originate a "very rapid" signal [109, 126]. When it is formed, the "very rapid" signal is originated from a catalytic intermediate [86, 107, 109, 113].

The structure of the "very rapid" signal-giving species was also probed by X-ray absorption (XAS) and electron nuclear double resonance (ENDOR) spectroscopies. Both supported the presence of a Mo=O group [121, 127] with ENDOR showing the presence of only one single ^{17}O-oxygen atom in the coordination sphere of molybdenum [128]. That earlier ENDOR study suggested the formation of a direct Mo-C(substrate) intermediate (Mo…C distance ≤ 2.4 Å) [128], but, later, Manikandan et al. in 2001 [129], assuming that the carbon undergoes a sp^2-hybridisation, suggested instead a Mo…C distance of 2.8 Å, a value similar to the one later observed in the crystallographic structure of the XO-FYX complex and consistent with a Mo-O-C(substrate) complex.

The structurally related XO-alloxanthine complex can, in a similar way, be formulated as **Mo^{5+}(=O_{axial})(=$S_{equatorial}$)-$N_{equatorial}$(alloxanthine)** (Fig. 3) and this structure was also confirmed by X-ray crystallography [130].

The "Rapid" Signals

The signals of the "rapid" type, originated also from XO molecules in the native, sulfo, form, can be easily distinguished from the "very rapid" by their rhombicity ($g_1 > g_2 > g_3$), by having $g_1 < 2$ and by the presence of hyperfine structure due to coupled protons (e.g., $g_{1,2,3}$ = 1.989, 1.969, 1.965, with 1-methyl-xanthine [115, 131]) (Fig. 3) [107, 131, 132]. The "rapid" signals can be obtained apparently with all substrates, within the turnover time. Noteworthy, they can be generated with substrates/reagents that do not reduce the enzyme through the molybdenum, as is the case of NADH (that reduces the XO through the FAD) or dithionite [110, 133–141]. Yet, they are not observed in single turnover assays with purinic substrates [113, 142, 143]. Moreover, the addition of xanthine causes very little changes in the signal [107, 134, 142], showing that the presence of the substrate has little influence in the coordination sphere of pre-reduced molybdenum and, thus, that the xanthine molecule does not become bound to the pre-reduced molybdenum. In compliance, no interaction with ^{13}C-labelled purinic substrate is observable in the "rapid" signals. Hence, in contrast to the "very rapid", the "rapid" signal-giving species does dot have the substrate bound and it does not represent a productive catalytic intermediary of the XO reaction [142].

The hyperfine interactions with ^{17}O and ^{33}S are in the "rapid" signals strong anisotropic and weak isotropic respectively (A_{av}(^{17}O) = 4.2, 8.3, 44.0 MHz [144–146] and $A_{1,2,3}$(^{33}S) = 9.5, 9.9, 9.9 MHz [104, 122], using formamide). The strong anisotropic hyperfine coupling to ^{17}O was initially taken as evidence for the presence of a terminal oxo group (Mo=O and not Mo-O-R, following the same reasoning described above for the "very rapid" signal). Yet, later studies showed, instead,

that the ^{17}O interaction could arise from a non-terminal oxygen, a Mo-OH group (further discussed below), in a ligand field that includes a "spectator", axial Mo=O group [97, 147]. The isotropic coupling to ^{33}S suggested a non-terminal sulfur (Mo-S-R and not Mo=S) in the signal-giving species and, contrary to the "very rapid" signal, that the unpaired electron is not delocalised over the sulfur atom. In addition, the strong and anisotropic interaction with ^{95}Mo and ^{97}Mo ($A_{1,2,3}(^{95}Mo)$ = 184, 74.0, 77.0MHz and $P_{1,2,3}(^{97}Mo)$ = 4.0, −2.0, −2.0 MHz, with coincident $\boldsymbol{P}$ and $\boldsymbol{A}$ tensors axes, but not coincident with the $\boldsymbol{g}$ axes (with Euler angles of $\alpha = 0°$, $\beta = 18°$ and $\gamma = 0°$); with formamide [104]) was also taken as evidence for a Mo-SH(-OH) structure [123, 148].

Also in contrast to the "very rapid", the "rapid" signals display hyperfine interactions with solvent-exchangeable protons and two types can be defined. In "rapid type 1", the molybdenum interacts with two non-equivalent protons (e.g., $A_{1,2,3}$ = 36.2, 38.3, 38.5 MHz and 11.1, 8.3, 5.5 MHz, with 1-methyl-xanthine [115, 131, 146]), while in "rapid type 2" it interacts with two equivalent protons (e.g., $A_{1,2,3}$ = 39.0, 42.0, 45.3 MHz and 27.9, 29.4, 37.5 MHz, with borate [122]) (Fig. 3). In the presence of xanthine, e.g., mixtures of the two types are usually obtained, but higher xanthine concentrations and lower pH values favour the "type 1" [132, 134].

Comparative studies of the "rapid type 1" signal with ^{33}S-labelled XO and 1-methyl-8-^{1}H-xanthine versus 1-methyl-8-^{2}H-xanthine, in ^{1}H versus ^{2}H-labelled water, showed that the strongest coupled proton is originated from the C8 carbon of the substrate molecule that was hydroxylated in the previous catalytic cycle and this proton was attributed to the sulfur atom of the molybdenum centre (Mo-S-H)[2] [91, 122, 131, 138, 149, 150]. The apparent incompatibility between the weak interaction with the sulfur (a molybdenum ligand) and the strong interaction with the proton (not a molybdenum ligand) can be explained by a non-linear Mo-S-H structure [122]. An angular Mo-S-H allows the sulfur atom to be located near the nodal plane of the ground-state orbital of the molybdenum (in a lower electron density site), with the hydrogen atom out of the nodal plane into a region of higher electron density. The weakly coupled proton of "rapid type 1" could reside in the oxygen or in a neighbouring protein group with which the oxygen forms an hydrogen bond [104, 144]. This interpretation was supported by the similarity of the EPR spectra of model compounds [151] and, because the "very rapid" does not show interaction with protons, the oxygen atom involved can not be the axial one.

The two strongly coupled protons in the "rapid type 2" signals have also been attributed to the Mo-SH and Mo-OH groups [114]. It has been suggested that the Mo-SH group holds a strongly coupled proton in both signal types and it is the relative position of the proton in the Mo-OH group relatively to the molybdenum that

[2] Although the ^{2}H has a nuclear magnetic moment different from zero ($I = 1$), in CW EPR the expected splitting ($2I + 1 = 3$) is not observable. The hyperfine interaction due to hydrogen is usually weak and the line splitting due to ^{2}H is only *ca* 15% of the splitting due to ^{1}H (calculated based on the ration of the values of nuclear g_n, which are 5.59 and 0.86 for ^{1}H and ^{2}H, respectively). Hence, in practice, in CW EPR, ^{1}H substitution by ^{2}H "removes" the previous observable split by 2 ($2I + 1/2 = 2$).

determines if that proton is weakly ("rapid type 1") or strongly ("rapid type 2") coupled. Thus, following the same line of thinking used to rationalise the weak interaction with the sulfur and the strong interaction with the proton in the "rapid type 1" signal, the stronger interaction in the "rapid type 2" is due to a different geometry of the molybdenum centre and not to a molybdenum centre with a different structure.

Although the hyperfine interactions (with protons, sulfur, oxygen and carbon) are different in "very rapid" and "rapid" signals, reflecting changes in the geometry of the molybdenum centre, the relative position of the direct molybdenum ligands must remain unchanged and the basic structure of the "very rapid" signal-giving species can be here used as template. Hence, the structure of "rapid" signal-giving species suggested by the EPR data is a $\mathbf{Mo^{5+}(=O_{axial})(\text{-}SH_{equatorial})\text{-}OH_{equatorial}}$ complex, with the Mo-OH proton being present in different orientations in "type 1" and "type 2" signals (Fig. 3).

The "Slow" Signal

The "slow" signal is originated from XO molecules in the desulfo form, where the sulfo group, Mo=S, was substituted by an oxo group, Mo=O. Although this signal-giving species is not catalytically relevant (because "desulfo" molecules do not have hydroxylase activity), it is physiologically relevant (because it is present in cells) and its study provides further relevant structural information (confirmation). The signal could be obtained apparently with any substrate/reductant provided that "desulfo" enzyme molecules are present. Swann and Bray, in 1972 [136], demonstrated with xanthine-reduced XO that the formation of the "slow" signal is dependent on the slow intermolecular electron transfer, from reduced "sulfo" enzyme molecules to oxidised "desulfo" molecules. The lower reduction potential of the "desulfo" molybdenum centre (≈100 mV lower than the "sulfo" centre value [152]) further challenges its reduction [153]. Swann and Bray [136] demonstrated also that NADH (that reduces the XO through the FAD) is able to reduce both the "sulfo" and the "desulfo" enzyme molecules, leading to the simultaneous arising of "rapid" and "slow" signals. Moreover, the intensity of "rapid" and "slow" signals is proportional to the concentration of "sulfo" and "desulfo" XO molecules, respectively. Hence, the "desulfo" enzyme molecules can be reduced either by intermolecular electron transfer or by direct reduction and the co-presence of "rapid" and "slow" signals can be observed with any substrate/reductant (e.g., xanthine, NADH or dithionite [136, 141, 152–155]), as long as sufficient time is giving for the reduction to occur.

The "slow" signal is characterised by the presence of hyperfine structure due to two non-equivalent protons ($A_{1,2,3}$ = 44.7, 44.4, 42.6 MHz and 3.9, 4.5, 6.3 MHz, with dithionite) and by a lower g_{av} value ($g_{1,2,3}$ = 1.972, 1.967, 1.955), which allows it to be easily differentiated from the "rapid type 1" signal (Fig. 3) [123, 131, 138, 148, 156, 157]. The lower g_{av} value was suggested to result from a lower spin-orbit coupling with the oxygen orbitals comparatively to the situation found in the "rapid"-giving species with its sulfur atom [104]. In fact, the "slow" signal-giving

species is thought to share the same geometry with the species that gives rise to the "rapid type 1", with the sulfur being substituted by an oxygen and with the strongly coupled proton being assigned to that oxygen atom (Mo-OH_{strong} and Mo-SH_{strong}, in "slow" and "rapid" signals, respectively) [138]. Studies with model compounds further supported this interpretation [151]. As expected, the "slow" signal displays hyperfine structure due to two coupled oxygen atoms (A_{av} = 28 MHz) [145]. Hence, the structure of "slow" signal-giving species suggested by the EPR data is a **Mo^{5+}(=O_{axial})(-$OH_{equatorial}$)-$OH_{equatorial}$** complex (Fig. 3).

Signals Obtained From Inhibited and Inactive Forms of Xanthine Oxidase

The group of signals originated from inhibited XO molecules, in the sulfo and desulfo forms, are, obviously, not catalytically relevant, but the information obtained from their study is important to complete the structural picture of the enzyme molybdenum centre.

The "inhibited" signal is originated from XO molecules in the native, sulfo, form in the presence of formaldehyde (methanal) or methanol, which are known to inhibit the enzyme. It is a rhombic signal, with $g_1 < 2$ ($g_{1,2,3}$ = 1.991, 1.977, 1.951), and displays hyperfine structure due to a single non-exchangeable proton ($A_{1,2,3}$ = 12.3, 10.8, 15.3 MHz) (Fig. 4) [108, 122, 145, 158]. Generation of the "inhibited" signal with ^{2}H-labelled formaldehyde showed that the coupled proton is derived from the inhibitor and the use of ^{13}C-labelled formaldehyde ($A_{1,2,3}(^{13}C)$ = 52.5, 40.6, 40.6 MHz [108, 128]) suggested that the formaldehyde is coordinated to the molybdenum, probably in a bidentate mode [159] (Fig. 4). A more recent ENDOR study revealed that both protons of the formaldehyde moiety do interact with the molybdenum, but one of the couplings is too weak to be observed by standard CW EPR [160]. In accordance, it is proposed that the formate moiety becomes bound to the molybdenum, through a stable Mo^{5+} complex (Fig. 4), thus preventing the turnover and inhibiting the enzyme.

On the contrary, the "desulfo-inhibited" signal is originated from desulfo XO molecules. The "desulfo-inhibited" signal is obtained by developing, first, the "slow" signal in the presence of dithionite and, subsequently, adding ethylene-glycol (HO-CH_2-CH_2-OH) [161]. This denomination is derived from the XO form that gives rise to the signal ("desulfo") and its subsequent resistance to both oxidation and reduction ("inhibited"). It is also a rhombic signal, with $g_1 < 2$ ($g_{1,2,3}$ = 1.980, 1.973, 1.967); it does not display hyperfine structure due to protons, but it is coupled to two oxygen atoms (A_{av} = 5.5 MHz) [145, 161]. The "desulfo-inhibited" signal-giving species has been suggested to hold the ethylene-glycol moiety coordinated to the molybdenum, probably, also in a bidentate mode (Fig. 4).

The "arsenite" signal is obtained in the presence of arsenite, a XO inhibitor that binds particularly tightly to reduced XO [162, 163]. The signal is formed from reduced enzyme molecules either in the sulfo or desulfo form and displays strong anisotropic hyperfine and quadrupole coupling to the ^{75}As nucleus (I = 3/2 naturally present in 100%; $A_{1,2,3}(^{75}As)$ = −40, 128, −90 MHz and $P_{1,2,3}(^{75}As)$ = 27, −17,

−10 MHz) [162–165]. The signal is modified by xanthine, suggesting that the enzyme active site retains the ability to bind substrates in the presence of the inhibitor. Based on the known affinity of arsenite for thiols, it was suggested that arsenite binds to the reduced molybdenum center through its sulfo group, Mo-S-AsO_2^{2-} (Fig. 4).

The structure of the "arsenite" signal-giving species was also probed by XAS spectroscopy that suggested a non-linear Mo-S-As moiety (angle of ca 80°), with a Mo…As distance of 3.02 Å, and one of the arsenite oxygen atoms possibly bound to the molybdenum in the position of the equatorial Mo-OH (Fig. 4) [166]. The recent crystal structure of arsenite-inhibited XO clearly demonstrate the arsenite bidentate binding mode, involving the catalytically essential sulfo group and the equatorial labile oxygen atom [167], thus explaining the particularly tight binding of arsenite to reduced XO and the enzyme inhibition.

The "mercurial" signal is obtained when native, sulfo, XO is treated with *p*-chloro-mercuri-benzoate [168]. This thiol-modifying reagent reacts with the Mo-SH group of reduced XO, blocking it in a Mo-S-Hg-R complex, to yield an inactive XO form. This enzyme form gives rise to a rhombic signal ($g_{1,2,3}$ = 1.969, 1.958, 1.943) that does not display hyperfine structure due to coupled protons (Fig. 4) [168]. When the signal is generated in the presence of ^{199}Hg(I = 1/2)-labelled *p*-chloro-mercuri-benzoate a strong and anisotropic coupling is observable ($A_{1,2,3}$(^{199}Hg) = 443, 285, 272 MHz). The also strong and anisotropic coupling to ^{17}O ($A_{1,2,3}$(^{17}O) = 4.1, 8.2, 34 MHz) and ^{33}S ($A_{1,2,3}$(^{33}S) = 13.8, 7.4, 8.7 MHz), further supports the presence of a **Mo^{5+}(=O_{axial})(=$O_{equatorial}$)-$S_{equatorial}$-Hg(chloro-benzoate)** complex in the "mercurial" signal-giving species (Fig. 4).

Magnetic Interactions Within Xanthine Oxidase

XO holds two [2Fe-2S] centres and one FAD, besides the molybdenum centre. The two Fe/S centres, diamagnetic in the oxidised state ($[2Fe\text{-}2S]^{2+}$), can be spectroscopically discriminated upon reduction by one electron ($[2Fe\text{-}2S]^{+}$) to yield two S = 1/2 signals, called Fe/S I and II, with different g anisotropy and spin-relaxation rate [154, 169]. The Fe/S I signal, similar to the one spinach ferredoxin, displays lower g anisotropy ($g_{1,2,3}$ = 2.022, 1.932, 1.894) and, due to its slower spin-relaxation rate, can be observed at higher (liquid nitrogen) temperatures, comparatively to the Fe/S II signal ($g_{1,2,3}$ = 2.110, 1.991, 1.902, observed below 25 K, with unusual very broad linewidths). The one-electron reduced flavin gives rise to an isotropic S = 1/2 signal, with a linewidth of 1.94 mT characteristic of the neutral semiquinone radical, $FADH^{\bullet}$ [107, 154].

Because XO holds four redox-active centres, magnetic interactions between them are possible and expected. The magnetic interactions in XO have been studied since the 1970s, when the magnetic interaction between the Mo^{5+} and the Fe/S I was described for the first time: Ehrenberg, Anger and Bray observed that the "rapid" and "slow" signals are modified when the temperature is decreased [170]. In 1972, Lowe et al. [170] systematically studied the "slow" signal and

concluded that its splitting is dependent on the presence and intensity of the signal originated by the Fe/S I, resulting from a spin-spin isotropic coupling of 1.1 mT (40 K). Yet, the predicted splitting of the signal from the reduced Fe/S I could not be observed. Later, Lowe and Bray [171], studying the "desulfo inhibited" signal, obtained a larger spin-spin coupling ($d_{1,2,3}$ = 2.2, 2.4, 2.6 mT) that allowed the corresponding splitting of the Fe/S centre signal to be also observed, thus providing positive identification of this Fe/S centre as the interacting species with the molybdenum. Similar magnetic interactions, whose intensity is dependent on the Mo^{5+} signal type (ranging from 0.7 mT for the "rapid" to 2.4 mT for the "desulfo inhibited"), were also described in turkey, *Veillonella alcalescens* [171] and rat liver XO [141], in *P. putida* quinoline 2-oxidoreductase [172], or in *D. gigas* AOR [173, 174].

Other magnetic interactions in XO were described by Rupp et al. [175] and Barber et al. [176], namely between Mo^{5+} and Fe/S I (identified as a 100-fold increase in the power necessary to saturate the Mo^{5+} signal in the presence of reduced Fe/S I, at 103K), Fe/S I and Fe/S II (2.5-fold increase in the power necessary to saturate the Fe/S I signal in the presence of reduced Fe/S II, at 20 K) and between FAD and Fe/S I and between FAD and Fe/S II (70-fold increase in the power necessary to saturate the $FADH^{\bullet}$ signal in the presence of reduced Fe/S centres, at 173 K). No interactions were described between Mo^{5+} and $FADH^{\bullet}$ or between Mo^{5+} and Fe/S II [176].

The magnetic interactions detected are in complete agreement with the structure of XO that shows that the four redox-active centres are aligned in an almost linear fashion, defining an intramolecular electron transfer pathway that delivers electrons from the molybdenum centre to the FAD, Mo → Fe/S I → Fe/S II → FAD [85]. Hence, it is the Fe/S centre that gives rise to the Fe/S I signal that is present in the nearer α-helical domain to the molybdenum center. Moreover, the distance between the Fe/S I centre and the molybdenum were estimated by Lowe and Bray to be 10–25 Å [171] and by Coffman and Buettner to be ≤14 Å [177], values that compare remarkably well with the distance determined in crystal structure, with Mo-Fe of 14.7 Å.

EPR Studies of Desulfovibrio Aldehyde Oxidoreductase

D. gigas AOR was first described by Moura et al. [178] and is believed to be an aldehyde scavenger, acting in a complex chain of electron transfer proteins that links the oxidation of aldehydes to the reduction of protons [179, 180]. *D. gigas* AOR was the first XO family member for which the crystal structure was determined [181–183]. It is structurally similar to mammalian XO, but it holds only two Fe/S centres (yet, when the AOR structure is represented with its putative physiological partner, one flavodoxin, it becomes clear that the structural homology with XO is preserved [184]).

D. gigas AOR gives rise to several Mo^{5+} signals, all similar to the ones of XO, as expected from two similar enzymes. After rapid reduction with benzaldehyde,

salicylaldehyde, acetaldehyde or dithionite, AOR gives rise to a "rapid type 2" signal, with the characteristic two interacting protons ($g_{1,2,3}$ = 1.988, 1.970, 1.964, $A_{1,2,3}(^{1}H)$ = 32.0, 45.8, 34.6 and 31.7, 17.4, 25.6 MHz), as demonstrated by assays with ^{2}H-labelled water; the signal intensity indicated the presence of 10–30% of sulfo enzyme molecules [179, 180, 185, 186]. The formation of the "rapid type 1" signal can be achieved, e.g., with di-hydoxy-benzaldehyde reduction (Fig. 5) [18]. Extended reduction with dithionite (20 min) elicits the "slow" signal that arises from the remainder desulfo enzyme molecules present in the sample ($g_{1,2,3}$ = 1.971, 1968, 1.958, where only one coupled proton was detected, $A_{1,2,3}(^{1}H)$ = 46.4, 44.1, 39.5 MHz) [179]. So far, no signal arising from a AOR-substrate or AOR-product complex was reported (no "very rapid"-like signal was yet described).

Recent crystallographic results and kinetic assays showing that AOR is not irreversible inhibited by cyanide led Santos-Silva et al. to suggest that the active AOR holds a molybdenum centre with an oxo group in place of the XO characteristic sulfo group, (Mo=O instead of Mo=S) and that AOR did not require the sulfo group for activity [187]. Yet, the XO family members susceptibility to cyanide is highly variable. This is the case of the nicotinate dehydrogenase (described in the following section) or the purine hydroxylase [188, 189] that require extensive treatments to inhibit the enzyme. Hence, it can not be excluded that AOR is also an enzyme that is highly resistant to cyanide inactivation. This supposition is in agreement with the observation of "rapid" signals that are well documented to arise from MoO_2S cores, thus demonstrating that sulfo enzyme molecules are present in the *Desulfovibrio* AOR samples. However, the small percentage of the sulfo enzyme molecules could have not been observed by crystallography, being identifiable only by EPR: EPR spectroscopy allows the observation of sulfo and desulfo molecules (depending on the reductant and time of reduction; see discussion in XO, section "The "slow" signal"), while crystallography only shows the dominant fraction of desulfo enzyme molecules.

The inhibitory effect of arsenite was also evaluated in AOR. The "arsenite" signal obtained is analogous to the XO one ($g_{1,2,3}$ = 1.979, 1.972, 1.922, $A_{1,2,3}(^{75}As)$ = 60, 136, 120 MHz, $P_{1,2,3}(^{75}As)$ = 19, −10, −9 MHz) and the crystal structure of the AOR-arsenite complex showed the arsenite ion bound, in a monodentate mode, to the molybdenum atom at the equatorial position occupied by the catalytically labile Mo-OH, **Mo-$O_{eqautorial}$-AsO_2(=$O_{equatorial}$)** (the absence of the Mo=S group hampering the bidentate mode seen in XO) [190, 191].

EPR Studies of Nicotinate Dehydrogenase and Carbon Monoxide Dehydrogenase

Finally, the EPR signals of two other XO family members, whose molybdenum centres are different from the one of XO, should be here considered, namely the EPR signals of nicotinate dehydrogenase and carbon monoxide dehydrogenase.

Some prokaryotic enzymes of the XO family, in place of the terminal sulfo group, Mo=S, have, instead, a terminal seleno group, Mo=Se, that is also essential for the catalytic activity (Fig. 1b) [192–195]. This is the case of the *E. barkeri* nicotinate

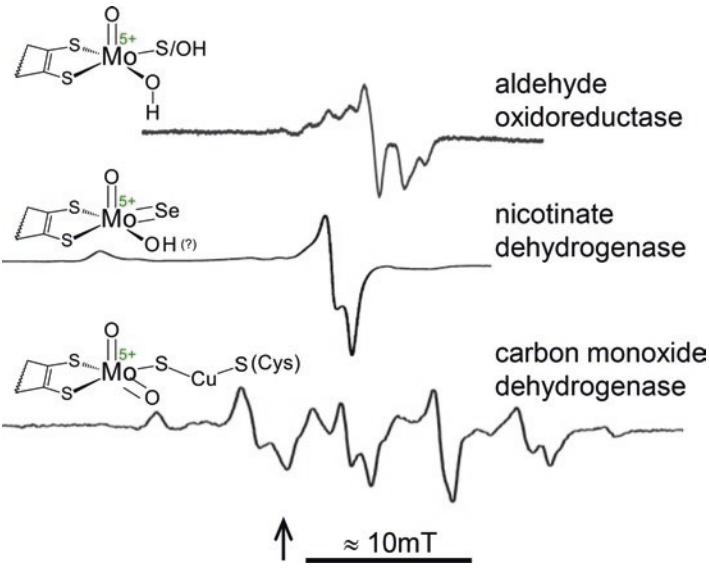

Fig. 5 Representative X-band EPR signals of aldehyde oxidoreductase, nicotinate dehydrogenase and carbon monoxide dehydrogenase and the respective structures proposed for each signal-giving species. The aldehyde oxidoreductase spectra is a mixture of "rapid" and "slow" signals and was obtained with dihydroxibenzaldehyde; adapted with permission from [18]. Nicotinate dehydrogenase "resting" (*as prepared*) signal; adapted with permission from [192], copyright (1994) National Academy of Sciences, U.S.A.. Carbon monoxide dehydrogenase signal obtained with carbon monoxide; adapted with permission from [200], copyright (2011) American Chemical Society. The *arrow* indicates the position of $g = 2.0037$

dehydrogenase, an enzyme that catalyses the hydroxylation of nicotinate to 6-hydroxy-nicotinate [192]. The reduced enzyme gives rise to an almost axial signal, with $g_1 \gg 2$ ($g_{1,2,3} = 2.067, 1.982, 1.974$ [192]), significantly higher than the g_1 value observed in the XO "very rapid" or "alloxanthine" signal (Fig. 5), as would be expected based on the higher covalency of the Mo-Se comparatively to a Mo-S. The signal is splitted when ^{77}Se($I = 1/2$)-enriched enzyme is used, showing that the selenium atom is located within magnetic contact to the molybdenum atom. Interestingly, the selenium-deficient enzyme (purified from selenium-deficient cells) gives rise to a Mo^{5+} signal similar to the "rapid type 1" of XO, suggesting that the molybdenum centres of nicotinate dehydrogenase and XO should be identical, apart from the replacement of Mo=S by Mo=Se, what was, in fact, recently confirmed when the crystallographic structure of the *E. barkeri* enzyme was determined [195].

Another "exception" to the characteristic XO molybdenum centre is provided by the Mo-S-Cu-S(Cys) binuclear centre of carbon monoxide dehydrogenase (Fig. 1b), an enzyme that catalyses the carbon monoxide oxidation to carbon dioxide [74–78]. This enzyme, upon reaction with carbon monoxide, gives rise to a unique Mo^{5+} signal, with $g_1 > 2$ ($g_{1,2,3} = 2.001, 1.960, 1.955$), that displays a strong anisotropic hyperfine coupling to one copper atom ($A_{1,2,3}$(Cu) = 117, 164, 132 MHz; $I = 3/2$ for both

^{63}Cu and ^{65}Cu, naturally present in ca 69 and 31%, respectively) (Fig. 5) [196–198]. A similar copper hyperfine interaction was observed in model complexes containing the Mo-S-Cu moiety [199]. When the signal is generated from carbon monoxide dehydrogenase molecules that were reconstituted with silver (after the sulfur and copper atoms had been removed by reaction with cyanide; the silver-substituted enzyme retains partially the activity [76, 200]), the expected splitted signal is observed ($A_{1,2,3}$(Ag) = 82.0, 78.9, 81.9 MHz; I = 1/2 for both ^{107}Ag and ^{109}Ag, naturally present in ca 52 and 48%, respectively) [200]. Moreover, the signal of CO-reduced enzyme in ^{1}H- or ^{2}H-labelled water displays no hyperfine coupling to protons, suggesting that this enzyme holds an equatorial deprotonated oxo group, Mo=O, contrary to XO with its labile Mo-OH group. Finally, the splitting of the Mo^{5+} signal, when ^{13}C-labelled carbon monoxide-reduced enzyme was used, demonstrated clearly that the carbon monoxide or dioxide is present in the signal-giving species of substrate-reduced enzyme [198]. Hence, the structure of the signal-giving species suggested by the EPR data is a **Mo^{5+}(=O_{axial})(=O)-S-Cu-S(cys)$_{equatorial}$** complex, with the carbon monoxide coordinated to the copper atom (thus, a paramagnetic enzyme-substrate complex analogue). This structure is supported (1) by the *O. carboxidovorans* enzyme crystallographic structure (the Mo-S-Cu-S(Cys) moiety) [75]; (2) by XAS studies that showed the presence of a two Mo=O groups and of an approximately linear Cu^{+} coordination [201]; (3) by resonance Raman spectroscopy, whose results are consistent with a $CuSMoO_2$ core [198, 201]; () and by a recent ENDOR study that, using ^{13}C-labelled carbon monoxide, showed an isotropic hyperfine coupling (A_{av}(^{13}C) = 17.3 MHz) that could arise only from a Mo^{+5}/Cu^{+}-CO species [202].

Sulfite Oxidase Family

The Enzymes

The active site of SO family enzymes (in its oxidised form; Fig. 1b) is closely related with the one of XO family, but with the distinctive feature of having the protein, through a cysteine residue, directly coordinated to the molybdenum. In these enzymes, the molybdenum centre displays the same square-pyramidal geometry, with one apical oxo group (Mo=O), but with the equatorial plane formed by two sulfur atoms of one pyranopterin cofactor molecule, one oxo group (Mo=O) and the cysteine sulfur atom (Mo-S(Cys)) [4–11, 203, 204]. This family comprises the prototype vertebrate (most studied chicken and human) liver SO (Eq. (8)), plant SO, diverse prokaryotic sulfite dehydrogenases and eukaryotic assimilatory nitrate reductases (NaR; enzymes involved in nitrate assimilation in plants, algae and fungi[3]), as well as *Escherichia coli* YedY or mammalian mitochondrial amidoxime

[3] It should be noted that the eukaryotic assimilatory NaR is distinct from any type of prokaryotic NaR enzymes, which are classified as members of the dimethylsulfoxide reductase family (Section

reducing component (mARC; enzymes involved in the reduction (dehydroxylation) of S- and N-hydroxylated compounds) and the MOSC proteins homologues (involved in molybdenum centre sulfuration) [71–73, 203–208].

Structurally, the vertebrate SO is an homodimeric enzyme, with each monomer holding one *b*-type haem and one molybdenum centre [209]. Being a key enzyme in the catabolism of sulfur-containing amino acids and other compounds, vertebrate SO catalyses the oxidation of the toxic sulfite to sulfate, at the molybdenum centre (Eq. (9)), with the simultaneous reduction of cytochrome *c*, at the *b*-type haem [210]. Surprisingly, the crystal structure of vertebrate (chicken) SO showed that the molybdenum and haem centres are more than 30 Å apart [209]. Hence, during catalysis, a conformational alteration would have to take place, to bring the two centres into sufficiently close proximity as to allow rapid intramolecular electron transfer observed, (sulfite→)Mo→haem(→cytochrome *c*) [211–213].

The members of the SO family, in contrast to XO family enzymes, are thought to be proper oxo-transferases, catalysing the simple transfer of an oxygen atom to, or from, a lone electron pair of the substrate, as is clearly exemplified by the SO-catalysed sulfite oxidation to sulfate (Eq. (9)) and NaR-catalysed nitrate reduction to nitrite (Eq. (10)), respectively [4–11, 203, 204]. However, the recent identification of mammalian mARC and bacterial YedY, YcbX or YiiM, as well as several other MOSC proteins homologues (most of these not yet characterised), demonstrated that SO family enzymes are also involved in the reduction of S- and N-hydroxylated compounds and in sulfuration reactions.

$$SO_2^{2-} + H_2O + 2cyt.c\left(Fe^{3+}\right) \rightarrow OSO_2^{2-} + 2cyt.c\left(Fe^{2+}\right) + 2H^+ \tag{8}$$

$$SO_2^{2-} + H_2O \rightarrow OSO_2^{2-} + 2e^- + 2H^+ \tag{9}$$

$$ONO_2^- + 2e^- + 2H^+ \rightarrow NO_2^- + H_2O \tag{10}$$

The molecular mechanism of SO-catalysed sulfite oxidation is presently well understood (Fig. 6) [209, 214–222]: (1) catalysis is initiated at the oxidised molybdenum centre by nucleophilic attack of the sulfite lone-pair of electrons on the catalytically labile equatorial oxo group of the molybdenum (Mo^{6+}=O); this results in the formation of a covalent Mo^{4+}-O-SO_3 intermediate, where the molybdenum atom has become reduced by two electrons; (2) the presence of the "spectator" axial oxo group facilitates the subsequent cleavage of the Mo-O(substrate)$_{equatorial}$ bond (weakens it); product (sulfate) is then released to yield a Mo^{4+}-$OH_{(2)}$ core (the oxidation half-reaction); (3) finally, the two electrons transferred from the substrate to the molybdenum are intramolecularly transferred, one at a time, to the haem, where cytochrome *c* (the physiological partner) will be reduced, and the initial Mo^{6+}=O core is regenerated (reduction half-reaction).

"Dimethylsulfoxide Reductase Family").

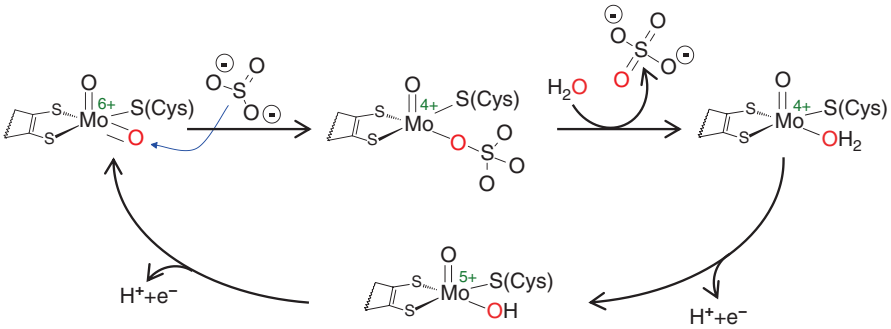

Fig. 6 Mechanism of sulfite oxidase-catalysed reaction. See text for details

In SO enzymes with one one-electron redox center (one haem in the case of chicken and human SO), the formation of a transient Mo^{5+} species is mandatory: the two electrons of Mo^{4+} must be, one at a time, transferred to the haem; after the haem being reduced by the first electron, it must wait for the physiological oxidising partner to be re-oxidised; only then, is able to receive the second electron. Hence, as in the XO family, the intramolecular electron transfer (Mo → haem, in this case) is an integral aspect of catalysis in the enzymes with one one-electron redox center. On the contrary, in the plant SO, that is devoid of additional redox centres, the reduction half-reaction is also carried out at molybdenum centre (in this case, the reduction of dioxygen) [223]. Also as seen in XO family, water is the ultimate oxygen atom donor/acceptor (Eqs. (9) and (10)) and the molybdenum centre mediates the oxygen atom transfer ($Mo^{6+}{=}O_{equatorial}$ is the direct oxygen donor and Mo^{4+} the oxygen acceptor).

EPR Studies of Vertebrate Sulfite Oxidase

Chicken SO is the best studied member of this family, with the human enzyme following closely, and this chapter will focus only the vertebrate enzymes (Fig. 7).

SO was the fifth enzyme discovered to contain molybdenum (after XO, AO, NaR and nitrogenase). The presence of molybdenum in bovine liver SO was revealed by Cohen, Fridovich and Rajagopalan, in 1971 [224], using EPR spectroscopy. Yet, comparatively to XO, the knowledge about SO advanced more slowly with relevant data being added only in the last decade.

Three Mo^{5+} EPR signals were early identified [224–230]. Generated by SO reduction with sulfite under low pH and high pH conditions and in the presence of phosphate, an inhibitor of the sulfite oxidising activity, they were designated “low pH” signal, “high pH” signal and “phosphate-inhibited” signal, respectively (Fig. 7). The “sulfite” signal was described by Bray et al. in 1982 [231], who pointed out its similarity with the “phosphate-inhibited” signal—both of which are now considered to arise from a family of similar signal-giving species, holding the anion coordinated via an oxygen atom to the molybdenum.

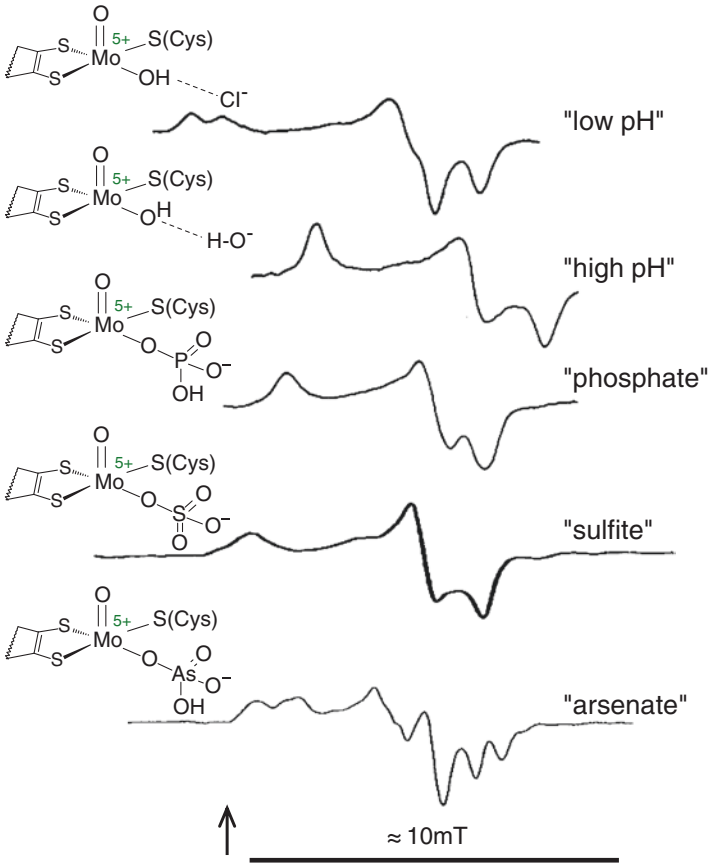

Fig. 7 Representative X-band EPR spectra of sulfite oxidase Mo^{5+} "low pH", "high pH", "phosphate", "sulfite" and "arsenate" signals and the respective structures proposed for each signal-giving species. "Low pH" signal obtained from sulfite-reduced SO at pH 6.5; adapted with permission from [230]. "High pH" signal obtained from sulfite-reduced SO at pH 10; adapted with permission from [230]. "Phosphate" signal obtained from sulfite-reduced SO, in the presence of phosphate buffer at pH 7.3; adapted with permission from [230]. "Sulfite" signal obtained from sulfite-reduced SO, at pH ≈ 6.4; adapted with permission from [231]. "Arsenate" signal obtained from sulfite-reduced SO, in the presence of arsenate at pH 6.5; adapted with permission from [260], copyright (1998) American Chemical Society. The *arrow* indicates the position of $g = 2.0037$

The "Low pH" Signal

The "low pH" signal, originated at moderately low pH values, is a rhombic signal, with $g_1 > 2$ ($g_{1,2,3}$ = 2.004, 1.972, 1.966), that displays strong coupling to one exchangeable proton ($A_{1,2,3}$ = 23.8, 22.1, 35.8 MHz) (Fig. 7) [229, 230]. More recently, it was also identified the coupling arising from the non-exchangeable proton of the Cα of the cysteine residue coordinated to the molybdenum atom ($A_{1,2,3} \approx$ 4, 6, 4 MHz) [232]. In the presence of ^{17}O-labelled water, the "low pH" signal

exhibits strong coupling to a solvent-exchangeable oxygen [124], which, based on resonance Raman spectroscopic data, was assigned to the equatorial Mo-OH group [233]. A weak coupling to a solvent-exchangeable oxygen was also described in the human SO mutant where the key arginine 160 residue was replaced by a glutamine (Arg160Gln), in the presence of ^{17}O-labelled water [234]. Recently, this oxygen was attributed to the sulfite moiety bound to the molybdenum (Mo-OSO_3^-) [235, 236].

The interaction of chloride, an inhibitor of the vertebrate SO, on the signal-giving species was studied in the pH range of 6.2–9.6 [237]. Interestingly, it was found that the interconversion between the "low pH" and "high pH" signal is influenced by the chloride concentration, with higher concentrations favouring the "low pH" signal (that is, increasing the apparent conversion pK_a by 1 pH unit). Initially, it was proposed that chloride would be directly coordinated to the molybdenum [237] in an equatorial position [238, 239]. However, a more recent analysis of the ^{35}Cl and ^{37}Cl quadrupole interaction showed that, while the hyperfine coupling is within the range expected for coordinated chloride, the nuclear quadrupole coupling observed in SO is very close to that expected for free chloride [240]. Hence, supported by DFT calculations (that showed that the quadrupole coupling, contrary to the hyperfine coupling, is very sensitive to the centre structure), it was concluded that chloride is bound in the substrate binding pocket, near the molybdenum, but not directly bound to the molybdenum atom itself [240]. This interpretation is in agreement with the crystallographic structure of the chicken enzyme, that shows one chloride ion in the substrate binding pocket [241], and further confirmed by a recent XAS spectroscopic study with bromide and iodide that suggested a halide-molybdenum distance of 5 Å [242].

If an increase in chloride concentration favours the "low pH" signal, its depletion results in a new signal, with different g values and $g_1 < 2$ ($g_{1,2,3}$ = 1.999, 1.972, 1.963) and without the strong proton coupling [243], similar to that characteristic of the "blocked" form of SO [234, 244]. The "blocked" signal-giving species holds the sulfite moiety bound to the equatorial catalytic labile oxo group of the molybdenum (Mo-$O_{equatorial}$-SO_3^-) in a trapped complex, as shown by pulsed EPR spectroscopy with ^{17}O and ^{33}S labelling [234, 243–245]. Noteworthy, the subsequent addition of chloride causes the disappearance of the "blocked" signal, release of sulfate and the formation of the characteristic "low pH" signal [243]. It was, thus, proposed that chloride favours the cleavage of the Mo-OSO_3^- bond to yield sulfate and a Mo-OH moiety, which would give rise to the "low pH" signal with its coupled proton.

Noteworthy, the human SO Arg160Gln mutant remains in the "blocked" form [234, 246], even upon addition of chloride [243], holding sulfite/sulfate coordinated to the molybdenum (Mo-O-SO_3^-) [234]. This suggests that the product release in this mutant is very slow or hampered, which, together with its striking decreased intramolecular electron transfer rate, seems to be the base of the lethality of this mutation [234, 241, 243].

The mutation of the cysteine that coordinates the molybdenum to a serine residue, in recombinant rat SO (Cys207Ser), was also studied [247]. The oxidised molybdenum centre of the mutant, which displays a 2000-fold decreased specific activity, is a MoO_3 core that, unexpectedly, does not have the serine residue coordinated to it, as revealed by XAS spectroscopy [248] and further confirmed by the

crystal structure and XAS of the mutant chicken SO [249]. Upon reduction, the serine becomes coordinated to the molybdenum, to give a Mo=O(-OH)-O(Ser) core, which gives rise to another EPR signal, with different g values and $g_1 < 2$ ($g_{1,2,3}$ = 1.979, 1.965, 1.955) and with a weaker proton coupling ($A_{1,2,3}$ = 6, 12, 6 MHz), comparatively to the wild-type SO [250].

On the contrary, the replacement of the molybdenum-coordinating cysteine by a selenocysteine residue resulted in a signal with an higher g_1 value ($g_{1,2,3}$ = 2.022, 1.975, 1.964), consistent with the higher covalency of the Mo-Se comparatively to a Mo-S (as describe above for the comparison between XO and nicotinate dehydrogenase; section "EPR Studies of Nicotinate Dehydrogenase and Carbon Monoxide Dehydrogenase") and with the known sensitivity of g_1 to modifications of equatorial plane of the molybdenum centre [251]. As expected, the new signal is also coupled to one proton ($A_{2,3}$ = 20, 35 MHz) [251].

The "High pH" Signal

The "high pH" signal, originated at higher pH values, is a rhombic signal, with $g_1 < 2$ ($g_{1,2,3}$ = 1.987, 1.964, 1.953), that, contrary to the "low pH" signal, was described as not having hyperfine structure due to coupled protons (Fig. 7) [229, 230]. However, a later ENDOR study demonstrated the presence of a solvent-exchangeable, strongly and anisotropically coupled proton in this signal, which was also assigned to the equatorial Mo-OH group [252–254]. Different orientations of the proton in the non-linear Mo-O-H group relatively to the molybdenum have been evoked to explain its different coupling in the "low pH" and "high pH" group, with the hydrogen located "in" the ground-state orbital of the molybdenum and "out" of that orbital, respectively. The coupling arising from the non-exchangeable proton of the Cα of the cysteine residue coordinated to the molybdenum atom was also identified in the "high pH" signal [232].

The "high pH" signal displays, as the "low pH" signal, strong coupling to a solvent-exchangeable oxygen, when in the presence of ^{17}O-labelled water) [124], which was assigned to the equatorial Mo-OH group [233]. In addition, the "high pH" signal shows weak coupling to a second oxygen atom ($A_{av}(^{17}O)$ = 6.4 MHz, $P_{av}(^{17}O)$ = 1.5 MHz) [255], which was ascribed to the axial Mo=O group by comparison with the interaction observed in model complexes [147, 256].

Contrary to the "low pH", the depletion of chloride has no effect on the formation of the "high pH" signal-giving species [243] and the Arg160Gln mutation does not either change this signal [246]. Also the replacement of the molybdenum-coordinating cysteine by a selenocysteine causes almost no change in the "high pH" signal, with the most prominent effect being a modest increase in the g_2 value [251]. The small effect of having a selenocysteine at high pH (comparatively to the marked effect observed at low pH) is consistent with the lower covalency of the Mo-SeH bond at high pH (where increased ligand covalency results in higher g_1 values) [71, 257].

The Family of "Oxo-Anion" Signals

Similar signals can be obtained with some oxo-anions, at low pH and high anion concentrations, namely phosphate, arsenate and sulfite.

The so called "phosphate-inhibited" signal, originated in the presence of phosphate, an inhibitor of the sulfite oxidising activity, is a rhombic signal, with $g_1 < 2$ ($g_{1,2,3}$ = 1.992, 1.969, 1.974), that does not display hyperfine structure due to coupled exchangeable protons (Fig. 7) [229, 230, 258, 259]. As noted in 1982 by Bray et al. [231], sulfite gives rise to a similar rhombic signal (but with g_1 close to 2), with no observable proton coupling (Fig. 7) [231, 243, 245]. In addition, also arsenate was shown to elicit an analogous signal (Fig. 7) [260].

The signal obtained with sulfite in the absence of chloride was later designated as "blocked" and, as already mentioned above (section "The "low pH" signal"), described to arise from a Mo-OSO_3^- core. The phosphate and arsenate complexes are thought to arise from similar complexes. Studies of the ^{31}P [258, 259] and ^{75}As [260] interactions (I = 1/2 and I = 3/2, respectively, both naturally present in 100%) indicated that the anions are coordinated to molybdenum through one of their oxygen atoms (Fig. 7), with the nuclear electric quadrupole coupling of ^{75}As pointing to a nearly tetrahedral arsenate [260]. Hence, a family of similar signal-giving species, holding the oxo-anion coordinated via one oxygen atom to the molybdenum, can be defined (Fig. 7).

Dimethylsulfoxide Reductase Family

The Enzymes

The DMSOR family is the larger and more diverse of the three families, comprising enzymes with widely varying function, subunit composition and makeup of additional redox-active centres [11, 24, 261–265]. The enzymes from this family harbour the molybdenum atom coordinated by four sulfur atoms of two pyranopterin cofactor molecules, in a trigonal prismatic geometry. In the oxidised form, the coordination sphere is completed by oxygen and/or sulfur and/or selenium atoms in a diversity of arrangements (Fig. 1b); the molybdenum atom is most often directly coordinated by the polypeptide chain via aspartate, serine, cysteine or selenocysteine residue side chains (arsenite oxidase, having no coordination to the polypeptide chain, is one important exception with the molybdenum centre coordinated by an apical oxo group plus one oxo/hydroxyl group (Mo=O(-OH)), in a square-pyramidal coordination geometry [266–269]). The DMSOR family is constituted by only prokaryotic enzymes that play remarkably different functions, including DMSOR, three different types of NaR enzymes (dissimilatory membrane-bound enzymes, dissimilatory periplasmatic enzymes and assimilatory cytoplasmatic enzymes (see note 3)), arsenite oxidase, arsenate reductase, several different types of formate dehydrogenases (FDH), polysulfide reductase, acetylene hydratase and many other.

Matching that diverse functionality, these enzymes catalyse remarkably different reactions, namely (1) proper transfer of oxygen atom (e.g., DMSOR-catalyse DMSO reduction (Eq. (11)) or NaR-catalysed nitrate reduction (Eq. (10))), (2) transfer of hydrogen atom (reversible FDH-catalysed formate oxidation to carbon dioxide (Eq. (12)) or benzoyl-coA reductase-catalysed benzoyl-CoA reduction to cyclohexa-1,5-diene-1-carboxyl-CoA), (3) transfer of sulfur atom (e.g., polysulfide reductase-catalysed inorganic sulfur reduction to sulfide), (4) *simultaneous* oxidation and reduction (e.g., reductive dehydroxylation and concomitant oxidative hydroxylation catalysed by pyrogallol:phloroglucinol hydroxyltransferase) and (5) even hydration reactions (e.g., acetylene hydratase-catalysed hydration of acetylene to acetaldehyde, a non-redox reaction).

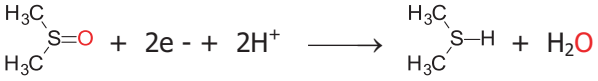

(11)

$$HCOO^- \rightarrow CO_2 + 2e^- + H^+ \tag{12}$$

To restrict the information presented to a manageable size, only two enzyme types from the DMSOR family will be described, namely the NaRs and FDHs.

Prokaryotes reduce nitrate to nitrite for dissimilatory and assimilatory processes and encode three distinct NaR enzymes [24, 270–278]: (a) membrane-bound cytoplasm-faced respiratory NaR, associated with the generation of a proton motive force across the cytoplasmatic membrane; (b) periplasmatic NaR, involved in the generation of a proton motive force or acting as an electron sink to eliminate excess of reducing equivalents; and (c) cytoplasmatic assimilatory NaR, involved in nitrogen assimilation. In spite of catalysing the same reaction (Eq. (10)), that occurs at the molybdenum centre, these enzymes have diverse subunit organisations and cofactor compositions and harbour different molybdenum centres. The three types of NaR enzymes have the molybdenum atom coordinated by the family characteristic two pyranopterin cofactor molecules (Fig. 1), but the remainder of the molybdenum coordination sphere is distinct in each enzyme type. In the respiratory membrane-bound NaR, the molybdenum atom is further coordinated by an aspartate residue in a bidentate fashion (that is, by the two oxygen atoms of its carboxylate), or alternatively by one terminal oxo group plus the aspartate residue coordinated in a monodentate mode (that is, by only one of its carboxylate oxygen atoms) [272, 279]. The two aspartate binding modes are thought to correspond to oxidised and reduced molybdenum centre. In the case of the periplasmatic NaR from *Desulfovibrio desulfuricans* or *Cupriavidus necator*, the molybdenum atom is coordinated instead by a cysteine sulfur atom plus one terminal sulfo group, forming a partial disulfide bond within each other [280–283]. Yet, the *E. coli* and *Rhodobacter sphaeroides* periplasmatic NaR, on their turn, complete the molybdenum coordination with the cysteine sulfur atom plus a terminal hydroxyl group [284, 285]. Finally, the cytoplasmatic assimilatory NaR, the least studied one, harbours its molybdenum atom coordinated by a cysteine residue [286].

The FDH enzymes are involved in different biochemical pathways, being also a structurally heterogeneous group of enzymes [24–26]. *E. coli*, e.g., expresses three FDHs: (a) a cytoplasmatic enzyme designated formate dehydrogenase H (FDH-H) [287] that is part of the formate-hydrogen lyase system and is involved in the oxidation of formate and generation of molecular hydrogen formation under fermentative (anaerobic) growth conditions [24, 288]; (b) a membrane-bound periplasm-facing FDH designated formate dehydrogenase N (FDH-N) that is part of the anaerobic nitrate-formate respiratory pathway (catalysed by a supermolecular formate:nitrate oxidoreductase system formed with the NaRGHI) involved with the generation of a proton motive force [264, 289–295]; and (c) a second membrane-bound periplasm-faced FDH, designated formate dehydrogenase O, that operates under aerobic conditions in another nitrate-formate respiratory pathway (this with the NaRZWV enzyme) [296–300]. In the case of FDHs, contrary to the above described NaRs, the molybdenum centre, where the reversible formate oxidation takes place (Eq. (12)), is more "uniform". Hence, these enzymes, in the oxidised form, have the molybdenum atom coordinated by two pyranopterin cofactor molecules and by a terminal sulfo group plus a conserved essential selenocysteine or cysteine residue (Mo=S(-Se(Cys)) or Mo=S(-S(Cys)); Fig. 1) [292, 301–309].

EPR Studies of Formate Dehydrogenases

The formate-reduced *E. coli* FDH-H gives rise to a nearly axial signal ($g_1 \gg g_2 \approx g_3$), with $g_1 = 2.094$ ($g_{2,3} = 2.001, 1.990$) that displays coupling to one solvent-exchangeable proton ($A_{1,2,3} = 7.5, 18.9, 20.9$ MHz), designated "2.094" signal (Fig. 8) [310, 311]. When the signal is generated from ^{77}Se-enriched enzyme a very strong and anisotropic interaction is observed ($A_{1,2,3}(^{77}\text{Se}) = 13.2, 75, 240$ MHz [312], values that are almost five times higher than the ones observed in Mo-Se model compounds [116, 312]). This interaction and the observation of the expected ^{95,97}Mo hyperfine coupling confirmed that the selenium atom of the selenocysteine is directly coordinated to the molybdenum and suggested that the unpaired electron is delocalised 17–27% over the selenium, once more supporting the covalency introduced by selenium in the Mo–Se bond [312].

Studies with ^{2}H-labelled formate (*E. coli* FDH-H) showed that the coupled solvent-exchangeable proton is originated from the substrate molecule [312]. It is worth mentioning that the proton coupling is absent in the beginning of reaction and it appears only in the following 30–300 s of reaction with formate [312]. The hyperfine interaction demonstrated that the proton acceptor is located within magnetic contact to the molybdenum center and photolysis assays showed that the selenium remains bound to the molybdenum and that it is not the proton acceptor (because in the photo-converted enzyme centre the interaction with ^{77}Se is not significantly affected, while the interaction with the proton disappears) [312]. Together, these results clearly demonstrate that the proton is transferred from formate Cα to the molybdenum center in the course of the catalytic turnover and, then, exchanged with the solvent. Based on these observations and on the crystallographic structure determined Boyington et al. [303]

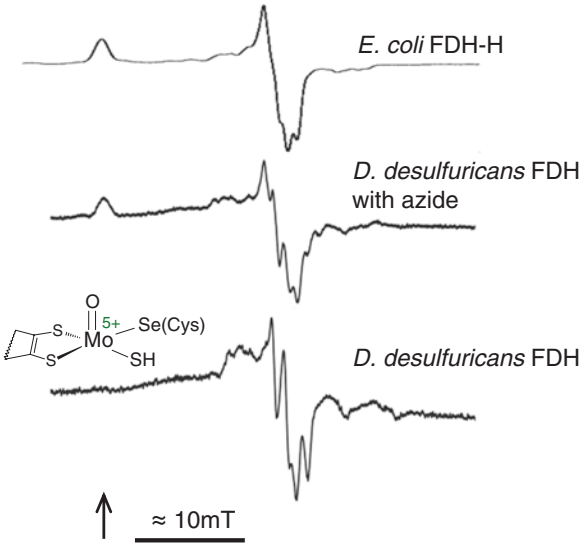

Fig. 8 Representative X-band EPR spectra of formate dehydrogenases. The *top spectrum* was obtained with formate-reduced *E. coli* FDH; adapted with permission from [312], copyright (1998) American Chemical Society. The *middle spectrum* was obtained from formate-reduced *D. desulfuricans* FDH in the presence of azide; adapted with permission from [307]. The *bottom spectrum* was obtained from formate-reduced *D. desulfuricans* FDH (without azide); adapted with permission from [307]. It is represented the signal-giving species structure proposed in [314, 315]. The *arrow* indicates the position of $g = 2.094$

and XAS data [313], Khangulov et al. [312] suggested that the *E. coli* FDH-H signal-giving species would have a Mo^{+5}-Se(Cys) core, with the coupled formate-derived proton residing on an amino acid residue located very close to the molybdenum (His_{141}). However, the subsequent identification of a sulfo group in the coordination sphere of the *E. coli* FDH-H molybdenum by Raaijmakers and Romão [306] (also confirmed by the identification of an *E. coli* sulfurtransferase that would insert the sulfur atom into the FDH molybdenum centre [308]), provided a more reasonable acceptor for the coupled formate-derived hydrogen: the Mo=S group that would be converted into a Mo-SH, thus, a direct molybdenum ligand being the proton acceptor [314, 315]. Hence, the suggested structure of the signal-giving species is a **Mo^{5+}-SH(-Se(Cys))** complex [314, 315] (Fig. 8).

The crystallographically proposed dissociation of the selenocysteine from the molybdenum coordination sphere by Raaijmakers and Romão [306] does not find support in none of the so far described EPR studies (nor in the *E. coli* enzyme EXAFS study at both the Mo and Se K-edges that indicated four or five Mo-S at 2.36 Å, plus one Mo-Se at 2.62 Å [313], or in the crystallographic structures of the *E. coli* FDH-N [292], *D. gigas* FDH [316]). It is possible that either the Mo^{5+} signal-giving species bears no relation to the species crystallographically observed or the crystallisation/irradiation induced some artefacts.

Subsequent studies by Rivas et al. [307] with the *D. desulfuricans* FDH demonstrated that the "2.094" signal only arises in the presence of azide, a strong FDH inhibitor (which was employed as a protective reagent during the *E. coli* FDH-H purifications). In fact, when the *D. desulfuricans* FDH is incubated with azide and reduced with formate or dithionite, the Mo^{5+} signals obtained showed almost identical *g* values and hyperfine structure to that described for the *E. coli* enzyme (Fig. 8) [307]. However, in the absence of azide, the formate or dithionite-reduced *D. desulfuricans* FDH gives rise to a rhombic signal with small anisotropy, with $g_{1,2,3}$ values of 2.012, 1.996, 1.985 [307]. The *D. desulfuricans* signal shows the expected hyperfine interaction with one solvent-exchangeable proton ($A_{1,2,3}$ = 23.1, 29.9, 27.8MHz) and an additional interaction with a second not solvent-exchangeable proton (A_1 = 35.1 MHz, $A_{2,3}$ not detectable) [307]. This later interaction arises from the selenocysteine Cβ hydrogen atoms [307], while the former, as discussed above for the *E. coli* enzyme, is assigned to the molybdenum sulfo group [314, 315].

With the *D. desulfuricans* enzyme, the studies with ^{2}H-labelled formate were inconclusive, because the $^{2}H/^{1}H$ exchange with the solvent is faster than the timescale of the "freezing technique" used. However, in the presence of the inhibitor azide, the reaction is decelerated and it was clearly shown that the formate Cα hydrogen is transferred, within 5 s, to a ligand of the molybdenum atom ($A_{2,3}$ = 21.0, 21.1 MHz, A_1 not determined) and, then, exchanged rapidly with the solvent [307]—thus, the strongly coupled proton is substrate-derived and, then, solvent-exchangeable. In this way, the EPR-supported structure for the signal-giving species is, once more, a **Mo^{5+}-SH(-Se(Cys))** complex [314, 315] (Fig. 8). Although the crystallographic structure of the *D. desulfuricans* FDH was not yet determined, the XAS results obtained suggested that both the oxidised and reduced molybdenum center is hexa-coordinated, with the selenocysteine and sulfo group bound to the molybdenum atom [317], thus supporting that signal-giving species structure.

Among other FDH enzymes, the NAD-dependent FDH from *Methylosinus trichosporium* and *Ralstonia eutropha* were also probed by EPR spectroscopy. The *M. trichosporium* enzyme displays a similar rhombic Mo^{5+} signal with small anisotropy ($g_{1,2,3}$ = 2.005, 1.091, 1.984) and well-resolved hyperfine structure due to $^{95,97}Mo$ [318]. This is also the case of the *R. eutropha* FDH Mo^{5+} signal ($g_{1,2,3}$ = 2.009, 2.001, 1.992 and $A_{1,2,3}(^{95,97}Mo)$ = 138, 82, 45 MHz) that displays strong isotropic coupling to one proton ($A_{1,2,3}(^{1}H)$ = 18, 21, 18 MHz) [314]. When the signal is generated in ^{2}H-labelled water, the proton hyperfine structure disappears, demonstrating the solvent-exchangeability of the proton. As observed in the *E. coli* and *D. desulfuricans* enzymes, studies with ^{2}H-labelled formate (in ^{1}H-water) confirmed that the solvent-exchangeable coupled proton is originated from the substrate molecule, with the coupling being absent in the beginning of the reaction and growing in over the course of 1 min of reaction, to yield a signal indistinguishable from that seen in the dithionite-reduced enzyme. Hence, additional proof that the proton is transferred from formate Cα to the molybdenum center in the course of the reaction and, then, exchanged with the solvent. Therefore, there is a general consensus that the structure of the signal-giving species in FDHs is a **Mo^{5+}-SH(-Se(Cys))**

complex [314, 315]. This consensus gives confidence to the recent proposal of the FDH reaction mechanism involving the hydride transfer from formate to the molybdenum sulfo group, Mo=S, to yield carbon dioxide and a Mo-SH core [314, 315].

Besides the studies above described, the EPR spectroscopy was also successfully used to probe the magnetic interactions between the redox-active centres of several FDH enzymes, as is the case of the enzymes from *M. trichosporium* [318], *Desulfovibrio* sp. [319] and *R. eutropha* [314]. Moreover, and most relevant, EPR spectroscopy was essential to demonstrate the incorporation of either molybdenum or tungsten in *D. alaskensis* FDH, one of the few examples of an enzyme that can incorporate either metal atoms and retain activity [319]. Metal quantification assays indicated that the *D. alaskensis* FDH is a mixture of two forms, one containing one molybdenum atom and the other one tungsten atom. Two EPR signals, typical of Mo^{5+} and W^{5+}, were observed. The Mo^{5+} signal is rhombic, with small anisotropy and $g_1 < 2$ ($g_{1,2,3}$ = 1.971, 1.968, 1.959) and displays hyperfine structure due to a coupled proton ($A_{1,2,3}$ = 44.2, 44.1, 43.9 MHz). The W^{5+} signal is also rhombic, but with lower and more anisotropic g values ($g_{1,2,3}$ = 1.955, 1.933, 1.916), as would be expected from the much stronger spin-orbit coupling in tungsten compared to molybdenum. Also because the CW EPR linewidths tend to be broader in tungsten compounds compared to molybdenum, no hyperfine structure is visible in the *D. alaskensis* FDH W^{5+} signal. The molybdenum substitution by tungsten was also studied in DMSOR (the substitution was forced; contrary to *D. alaskensis* FDH, the *Rhodobacter capsulatus* DMSOR does not incorporate tungsten naturally) [320]. Two different signals were observed, both rhombic, with higher g anisotropy, but, while one signal displays no visible hyperfine coupling to protons ($g_{1,2,3}$ = 1.958, 1.928, 1.860, $A_{1,2,3}(^{183}W)$ = 104, 108, 110 MHz), the other shows clear hyperfine coupling to one proton ($g_{1,2,3}$ = 1.960, 1.927, 1.888, $A_{1,2,3}(^{183}W)$ = 110, 108, 106 MHz, $A_{1,2,3}(^{1}H)$ = 35.7, 37.8, 52.9 MHz).

EPR Studies of Nitrate Reductases

Periplasmatic Nitrate Reductases Signals

Periplasmatic NaRs from different sources were investigated by EPR spectroscopy, including from *D. desulfuricans* [274, 321, 322], *Paracoccus pantothrophus* [323–326], *R. sphaeroides* [285, 327, 328], *E. coli* [284] and others [329, 330]. The Mo^{5+} of these enzymes can give rise to several EPR signals, designated "very high g", "high g", "high g-nitrate", "high g-turnover", "low g-unsplit" and "low g-split".

The "very high g" is a rhombic signal, with $g_1 > 2$ that is coupled to one proton ($g_{1,2,3}$ = 2.022, 1.999, 1.994, $A_{1,2,3}$ = 20.9, 20.7, 18.4 MHz, for the *P. pantothrophus* enzyme); it is thought to arise from an inactive form of the enzyme (Fig. 9) [323, 324, 328]. The "low g" signals are also rhombic, but with $g_1 < 2$ ($g_{1,2,3}$ = 1.997, 1.962, 1.959 and $g_{1,2,3}$ = 1.996, 1.969, 1.961, for the "low g-unsplit" and "low g-split" signals of the *P. pantothrophus* enzyme) and the "low g-split", as its name

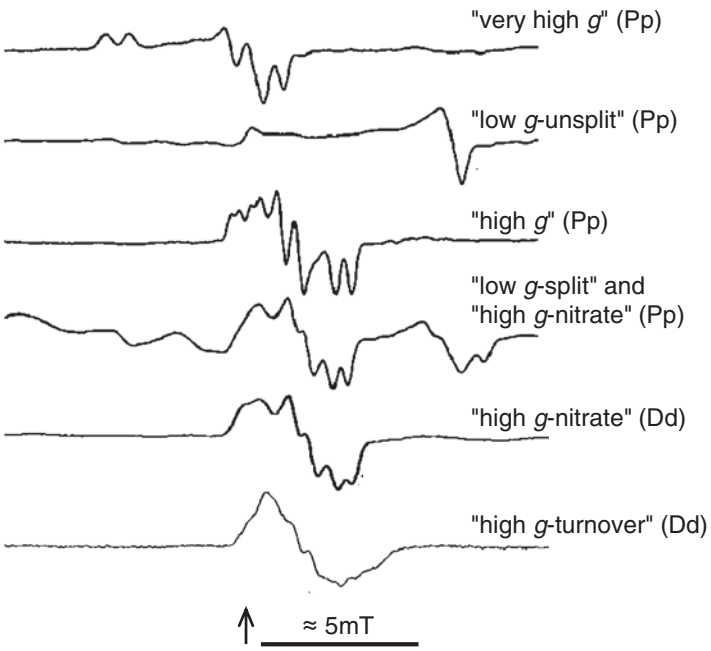

Fig. 9 Representative X-band EPR spectra of periplasmatic nitrate reductases. From *top* to *bottom*: "Very high *g*" signal obtained from cyanide-treated dithionite-reduced *P. pantothrophus* enzyme; adapted with permission from [324], copyright (1999) American Chemical Society. "Low *g*-unsplit" signal obtained from *P. pantothrophus* enzyme by prolonged incubation with dithionite; adapted with permission from [324], copyright (1999) American Chemical Society. "High *g*" signal was obtained from as-prepared, resting *P. pantothrophus* enzyme; adapted with permission from [324], copyright (1999) American Chemical Society. The fourth spectrum shows the "high *g*-nitrate" and "low *g*-split" signals obtained from dithionite-reduced *P. pantothrophus* enzyme that was reacted with nitrate; adapted with permission from [324], copyright (1999) American Chemical Society. "High *g*-nitrate" signal obtained from dithionite-reduced *D. desulfuricans* enzyme reacted with nitrate; adapted with permission from [321]. "High *g*-turnover" signal obtained from methyl-viologen-reduced *D. desulfuricans* enzyme reacted with nitrate; adapted with permission from [321]. The *arrow* indicates the position of $g = 2$

indicates, displays coupling to one proton ($A_{1,2,3}$ = 36.3, 37.5, 42.0 MHz) (Fig. 9) [323, 324, 328]. The "low *g*" signal is similar to the "rapid type 1" signal of XO and the signal-giving species is thought to hold the molybdenum atom coordinated by only one pyranopterin cofactor molecule. Furthermore, XAS results suggested the presence of at least one terminal oxo group [324]. Hence, the "low *g*-split" is also attributed to an inactive form of the enzyme.

The "high *g*" is a rhombic signal, with $g_1 < 2$ ($g_{1,2,3}$ = 1.999, 1.990, 1.981, for the *P. pantothrophus* enzyme) that displays weak coupling to two not solvent-exchangeable protons ($A_{1,2,3}$ = 17.9, 14.5, 13.9 MHz and A_1 = 8.4 MHz (*P. pantothrophus*)), which were assigned to the molybdenum-coordinated cysteine Cβ

hydrogen atoms (Fig. 9) [323–326]. While the "high *g*" signal does not change in the presence of nitrate (as well as, of nitrite or azide), a different signal, the "high *g*-nitrate" signal, is obtained after the addition of nitrate to dithionite-reduced enzyme under turnover conditions, which has lower *g* anisotropy and one (*D. desulfuricans*) or two (*P. pantothrophus*) coupled protons ($g_{1,2,3}$ = 2.000, 1.990, 1.981, $A_{1,2,3}$ = 12.9, 13.9, 12.8 MHz, for *D. desulfuricans* [321, 322]; $g_{1,2,3}$ = 1.999, 1.989, 1.982, $A_{1,2,3}$ = 17.9, 12.0, 12.8 MHz and A_1 = 9.0 MHz, for *P. pantothrophus* [324, 325]) (Fig. 9). If methyl-viologen-reduced enzyme is used instead, the addition of nitrate elicits a similar signal, designated "high *g*-turnover", that displays hyperfine structure due to two equivalent solvent-exchangeable protons ($g_{1,2,3}$ = 1.999, 1.992, 1.982, $A_{1,2,3}$ = 16.2, 18.1, 15.3 MHz, for *D. desulfuricans* [321, 322]) (Fig. 9). Assays with common (^{14}N) and ^{15}N-labelled nitrate excluded the possibility that these signals arise from Mo-ONO_2 complexes, thus questioning the catalytic relevance of the signals [321, 322, 326], even though this conclusion is not consensual [328].

Presently, it is clear that the spectroscopic characterisation of the periplasmatic NaR enzymes is far from being concluded and the structure of the various signal-giving species is still obscure, as is their catalytic relevance (compared, e.g., with the wealth of information regarding the several XO signals (section "Xanthine Oxidase Family")). A recent theoretical study provided a rationalisation for the structure of some signal-giving species [331]. The "very high *g*" signal and "high *g*" signals family are suggested to arise from MoS_6 cores, with the "high *g*" species considered to be the ones in the more reduced state (that is, the ones with the proposed persulfide bond between the sulfo group, Mo-S, and the cysteine sulfur, Mo-S(Cys), [322] reduced) [331]. The differences between the signals may arise from different distortions of the molybdenum coordination sphere and/or the presence of different ions in the close proximity of the molybdenum [332]. The "low *g*" signals are suggested to arise from molybdenum centres with only one pyranopterin molecule, as suggested before (and described above), with the molybdenum coordination sphere completed as a **Mo=X(-OH)(-S(Cys))** core, where X is an oxygen or sulfur atom [331].

Assimilatory Nitrate Reductases Signals

The assimilatory NaRs are the least well characterised of these enzymes, but their Mo^{5+} signals are quite similar to the ones of the periplasmatic homologues, consequence of the presence of one molybdenum-coordinated cysteine in both enzymes types. The assimilatory enzyme from *Azotobacter vinelandii* enzyme is known for long to give rise to a "very high *g*" and "high *g*-nitrate" signals [333]. Also the cyanobacterium *Synechococcus* sp. PCC 7942 assimilatory enzyme elicits a "very high *g*" ($g_{1,2,3}$ = 2.023, 1.998, 1.993) and "high *g*" signals ($g_{1,2,3}$ = 1.997, 1.990, 1.982), which are thought to arise from inactive and functional enzyme forms, respectively [286].

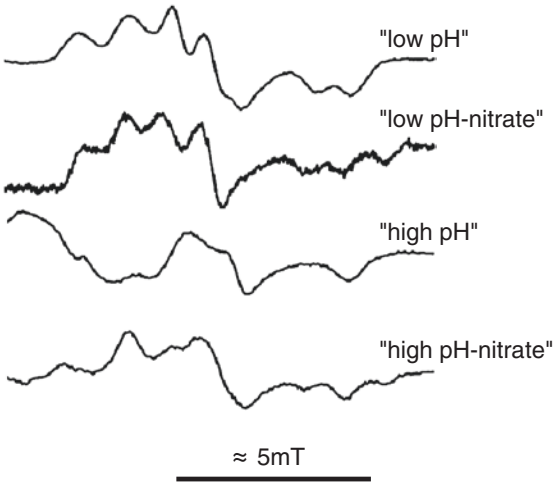

Fig. 10 Representative X-band EPR spectra of respiratory nitrate reductases from *D. desulfuricans*. "Low pH" signal obtained at pH 6.0. "Low pH – nitrate" signal obtained at pH 6.0 from dithionite-reduced enzyme treated with nitrate showing the "low pH – nitrate" signal plus a new rhombic signal. "High pH" signal obtained at pH 7.6. "High pH – nitrate" signal obtained at pH 6.0 from dithionite-reduced enzyme treated with nitrate showing the "low pH – nitrate" signal plus a new rhombic signal. All spectra were adapted with permission from [342]. The *arrow* indicates the position of $g = 2$

Respiratory Nitrate Reductases Signals

The Mo^{5+} of respiratory NaRs also give rise to several EPR signals, but distinct from the ones of the perplasmatic and assimilatory enzymes [334–342]. Two are pH-dependent and display hyperfine coupling to a solvent-exchangeable proton. The "low pH" is a rhombic signal, with $g_1 > 2$ ($g_{1,2,3} = 2.001, 1.986, 1.964$, $A_{1,2,3}(H) = 31.7, 23.6, 24.7$ MHz), while the "high pH" has a $g_1 < 2$ and a weaker hyperfine interaction ($g_{1,2,3} = 1.988, 1.981, 1.962$, $A_{1,2,3}(H) = 10.6, 8.9, 9.1$ MHz, for the *E. coli* enzyme) [338]. Similar signals have been since reported for the enzyme from *M. hydrocarbonoclasticus* enzyme (Fig. 10) [342], *Pseudomonas aeruginosa* [337] and others. Of note, the *P. pantothrophus* enzyme exhibits also "low pH" and "high pH" signals lacking resolved hyperfine coupling ($g_{1,2,3} = 2.007, 1.987, 1.970$ and $1.990, 1.989, 1.967$, respectively), which have been interpreted as arising form a different substrate binding mode [259, 338, 343–345]. The difference in the extent of coupling as a function of pH may arise from different orientations of the proton, in a non-linear Mo-O-H group, relatively to the molybdenum atom (as argued above for SO (section "Sulfite Oxidase Family")), or may be the result of different nitrate binding modes, as suggested for the *M. hydrocarbonoclasticus* enzyme [342]. Regarding the Mo-OH group, the "low pH" signals exhibits no ^{17}O hyperfine coupling in assays with ^{17}O-labelled water or ^{17}O-labelled nitrate, thus questioning the

presence of a Mo-OH group in that signal-giving species (although it is possible that a very weak coupling could have not been observed in standard CW EPR assays); the "high pH" signal, in assays with ^{17}O-labelled water, on the other hand, displays a weak hyperfine coupling ($A_{1,2,3}(^{17}O)$ = 5.5, 8.8, 5.5 MHz), suggesting a Mo=O group [346]. The catalytic significance of the "low pH" signal has been defended since the late 1970s [336, 340], but a later study [336, 340] suggested that both signal-giving species would be involved in the enzyme turnover.

The effect of different anions in the "low pH" signal has also been studied. Fluoride (I = 1/2, naturally present in 100%) elicits a well defined hyperfine interaction ($A_{1,2,3}(^{19}F)$ = 30.6, 15.3, 13.2 MHz (*E. coli*)), suggesting that the halide is bound very near the molybdenum atom (instead of being directly coordinated to the metal, as argued above for SO (section "Sulfite Oxidase Family")) [338]. Addition of nitrate or nitrite to the *E. coli* enzyme give rise to different signals, with $g_1 > 2$, all showing hyperfine coupling to protons ($A_{av}(^{1}H)$ = 34–36 MHz) [338]. Similar signals were obtained upon nitrate addition to dithionite-reduced *M. hydrocarbonoclasticus* enzyme ($g_{1,2,3}$ = 2.002, 1.987, 1968, $A_{1,2,3}(^{1}H)$ = 39.2, 30.6, 30.3 MHz), but in a pH-independent manner and with the simultaneous observation of a new rhombic signal that displays no hyperfine structure ($g_{1,2,3}$ = 1.996, 1.982, 1979) (Fig. 10) [342].

Concluding Remarks

EPR spectroscopy has contributed enormously and significantly to our present knowledge about molybdenum-containing enzymes. This is particularly true for mammalian XO, to which the huge number of EPR studies (together with other spectroscopic methodologies), were decisive to draw a picture of the molybdenum centre of XO family enzymes before the first crystal structure of a XO family member was available in 1995 (*D. gigas* AOR). The EPR spectroscopy contribution to validate the hydroxylation reaction mechanism was also decisive, with the demonstration of hydrogen transfer from the substrate to the molybdenum sulfo group, Mo=S, and transfer of the water oxygen to the catalytically labile equatorial oxo group, Mo-OH. The contribution of EPR (and other spectroscopies) has also been extremely significant to our understanding of the SO molybdenum centre and reaction mechanism, namely the formation of "blocked" species, the chloride role or the mutant-based lethality. Yet, several questions remain open, including what drives the "low pH"/"high pH" transition (which residues) and the exact structures of those signal-giving species. Numerous questions remain also open regarding the FDH and NaR enzymes, for which it is clear that the spectroscopic characterisation is far from being concluded and the structure of the various signal-giving species is still obscure, as is their catalytic relevance. Nonetheless, the knowledge and experience gathered with the "older" enzymes and diverse model compounds will be, for sure, decisive to guide the future spectroscopic characterisation of the enzymes that only now are starting to be thoroughly studied.

Besides the mechanistic and structural studies focused in this chapter, the EPR spectroscopy has also been extensively used to monitor redox titrations. The knowledge of the reduction potentials is essential to understand the intramolecular electron-transfer processes within enzymes with several redox-active centres or between enzymes and their redox partners. In these studies, an EPR signal is taken as a measure of a determined oxidation state/enzyme species; e.g., the XO "rapid" and "slow" signals were used as indicators to assist in the determination of the reduction potential of the sulfo and desulfo molybdenum centres. Also the study of magnetic interactions is decisive to establish/confirm the "intramolecular wire of redox-active centres" that is responsible for the intramolecular electron-transfer, as was illustrated with the XO "intramolecular wire" that delivers the electrons from the molybdenum centre to the FAD.

Hence, we hope that we have managed to transmit that CW EPR is still a very valuable spectroscopic tool for the study of molybdenum-containing enzymes (and other metalloenzymes), although advanced EPR-related methods would be, for certainly, decisive.

Acknowledgements This work was supported by the Unidade de Ciências Biomoleculares Aplicadas—UCIBIO which is financed by national funds from FCT/MEC (UID/Multi/04378/2013) and co-financed by the ERDF under the PT2020 Partnership Agreement (POCI-01-0145-FEDER-007728). LBM thanks Fundacão para a Ciência e a Tecnologia, MEC, for a fellowship grant (SFRH/BPD/111404/2015, which is financed by national funds and co-financed by FSE).

References

1. Palmer G (1985) Biochem Soc Trans 13:548
2. Zhang Y, Gladyshev VN (2008) J Mol Biol 379:881
3. Zhang Y, Rump S, Gladyshev VN (2011) Coord Chem Rev 255:1206
4. Hille R (1996) Chem Rev 96:2757
5. Hille R (2002) Trends Biochem Sci 27:360
6. Schwarz G, Mendel RR, Ribbe MW (2009) Nature 460:839
7. Hille R, Mendel R (2011) Coord Chem Rev 255:991
8. Mendel R, Kruse T (2012) Biochim Biophys Acta 1823:1568
9. Hille R (2013) Dalton Trans 42:3029
10. Hille R, Hall J, Basu P (2014) Chem Rev 114:3963
11. Maia L, Moura I, Moura JJG (2017) Molybdenum and tungsten-containing enzymes: an overview. In: Hille R, Schulzke C, Kirk M (eds) Molybdenum and tungsten enzymes: biochemistry. RSC Metallobiology Series No. 5. The Royal Society of Chemistry, Cambridge, pp 1–80. doi:10.1039/9781782623915-00001
12. Anbar AD, Knoll AH (2002) Science 297:1137
13. Zerkle AL, House CH, Cox RP, Canfield DE (2006) Geobiology 4:285
14. Scott C, Lyons TW, Bekker A, Shen Y, Poulton SW, Chu X, Anbar AD (2008) Nature 452:456
15. Glass JB, Wolfe-Simon F, Anbar AD (2009) Geobiology 7:100
16. Schoepp-Cothenet B, van Lis R, Philippot P, Magalon A, Russell MJ, Nitschke W (2012) Sci Rep 2:263
17. Zhang X, Sigman DM, Morel FMM, Kraepiel AML (2014) Proc Natl Acad Sci U S A 111:4782

18. Maia LB, Moura JJG (2011) J Biol Inorg Chem 16:443
19. Maia LB, Moura JJG (2014) Chem Rev 114:5273
20. Sparacino-Watkins CE, Tejero J, Sun B, Gauthier MC, Thomas J, Ragireddy V, Merchant BA, Wang J, Azarov I, Basu P, Gladwin MT (2014) J Biol Chem 289:10345
21. Maia LB, Moura JJG (2015) J Biol Inorg Chem 20:403
22. Maia LB, Pereira V, Mira L, Moura JJG (2015) Biochemistry 54:685
23. Wang J, Krizowski S, Fischer K, Niks D, Tejero J, Sparacino-Watkins C, Wang L, Ragireddy P, Frizzell S, Kelley EE, Zhang Y, Basu P, Hille R, Schwarz G, Gladwin MT (2015) Antioxid Redox Signal 23:283
24. Grimaldi S, Schoepp-Cothenet B, Ceccaldi P, Guigliarelli B, Magalon A (2013) Biochim Biophys Acta 1827:1048
25. Hartmann T, Schwanhold N, Leimkühler S (2014) Biochim Biophys Acta 1854:1090
26. Maia LB, Moura JJG, Moura I (2015) J Biol Inorg Chem 20:287
27. Akaba S, Seo M, Dohmae N, Takio K, Sekimoto H, Kamiya Y, Furuya N, Komano T, Koshiba T (1999) J Biochem 126:395
28. Seo M, Koiwai H, Akaba S, Komano T, Oritani T, Kamiya Y, Koshiba T (2000) Plant J 23:481
29. Seo M, Peeters AJ, Koiwai H, Oritani T, Marion-Poll A, Zeevaart JA, Koornneef M, Kamiya Y, Koshiba T (2000) Proc Natl Acad Sci U S A 97:12908
30. Huang DY, Furukawa A, Ichikawa Y (1999) Arch Biochem Biophys 364:264
31. Hille R (2005) Arch Biochem Biophys 433:107
32. Garattini E, Fratelli M, Terao M (2008) Cell Mol Life Sci 65:1019
33. Pryde DC, Dalvie D, Hu Q, Jones P, Obach RS, Tran TD (2010) J Med Chem 53:8441
34. Garattini E, Terao M (2011) Drug Metab Rev 43:374
35. Hille R, Nishino T, Bittner F (2011) Coord Chem Rev 255:1179
36. Swenson TL, Casida JE (2013) Toxicol Sci 133:22
37. Terao M, Romão MJ, Leimkühler S, Bolis M, Fratelli M, Coelho C, Santos-Silva T, Garattini E (2016) Arch Toxicol 90:753
38. Hille R, Nishino T (1995) FASEB J 9:995
39. Hesberg C, Haensch R, Mendel RR, Bittner F (2004) J Biol Chem 279:13547
40. Yesbergenova Z, Yang G, Oron E, Soffer D, Flur R, Sagi M (2005) Plant J 42:862
41. Hille R (2006) Eur J Inorg Chem 2006:1913
42. Nishino T, Okamoto K, Eger BT, Pai EF, Nishino T (2008) FEBS J 275:3278
43. Zarepour M, Kaspari K, Stagge S, Rethmeier R, Mendel RR, Bittner F (2010) Plant Mol Biol 72:301
44. Okamoto K, Kusano T, Nishino T (2013) Curr Pharm Des 19:2606
45. Kappler U, Bennett B, Rethmeier J, Schwarz G, Deutzmann R, McEwan AG, Dahl C (2000) J Biol Chem 275:13202
46. Di Salle A, D'Errico G, La Cara F, Cannio R, Rossi M (2006) Extremophiles 10:587
47. Denger K, Weinitschke S, Smits THM, Schleheck D, Cook AM (2008) Microbiology 154:256
48. Wilson JJ, Kappler U (2009) Biochim Biophys Acta 1787:1516
49. Vijayakumar K, Gunny R, Grunewald S, Carr L, Chong KW, DeVile C, Robinson R, McSweeney N, Prabhakar P (2001) Pediatr Neurol 45:246
50. Johnson JL (2003) Prenat Diagn 23:6
51. Sass JO, Gunduz A, Araujo Rodrigues Funayama C, Korkmaz B, Dantas Pinto KG, Tuysuz B, Yanasse Dos Santos L, Taskiran E, de Fátima Turcato M, Lam CW, Reiss J, Walter M, Yalcinkaya C, Camelo Junior JS (2010) Brain Dev 32:544
52. Carmi-Nawi N, Malinger G, Mandel H, Ichida K, Lerman-Sagie T, Lev D (2011) J Child Neurol 26:460
53. Schwarz G, Belaidi A (2013) Met Ions Life Sci 13:415
54. Schwarz G (2016) Curr Opin Chem Biol 31:179
55. Fraústo da Silva JJR, Williams RJP (2001) The biological chemistry of the elements – the inorganic chemistry of life. Oxford University Press, Oxford
56. Bjornsson R, Lima FA, Spatzal T, Weyhermueller T, Glatzel P, Einsle O, Neese F, DeBeer S (2014) Chem Sci 5:3096

57. Bjornsson R, Neese F, Schrock RR, Einsle O, DeBeer S (2015) J Biol Inorg Chem 20:447
58. Burgmayer SJN, Stiefel EI (1985) J Chem Educ 62:943
59. Harlan EE, Berg JM, Holm RH (1986) J Am Chem Soc 108:6992
60. Holm RH, Berg JM (1986) Acc Chem Res 19:363
61. Holm RH (1987) Chem Rev 87:1401
62. Holm RH (1990) Coord Chem Rev 100:183
63. Xiao Z, Young CG, Enemark JH, Wedd AG (1992) J Am Chem Soc 114:9194
64. Holm RH, Donahue JP (1993) Polyhedron 12:571
65. Scbultz BE, Gbeller SF, Muetterties MC, Scott MJ, Holm RH (1993) J Am Chem Soc 115:2714
66. Holm RH, Kennepohl P, Solomon EI (1996) Chem Rev 96:2239
67. Donahue JP (2006) Chem Rev 106:4747
68. Reichenbecher W, Schink B (1999) Biochim Biophys Acta 1430:245
69. Prisner T, Lyubenova S, Atabay Y, MacMillan F, Kroger A, Klimmek O (2003) J Biol Inorg Chem 8:419
70. Nagarajan K, Joshi HK, Chaudhury PK, Pal K, Cooney JJA, Enemark JH, Sarkar S (2004) Inorg Chem 43:4532
71. Yang J, Rothery R, Sempombe J, Weiner JH, Kirk ML (2009) J Am Chem Soc 131:15612
72. Pushie MJ, Doonan CJ, Moquin K, Weiner JH, Rothery R, George GN (2011) Inorg Chem 50:732
73. Giles LJ, Ruppelt C, Yang J, Mendel RR, Bittner F, Kirk ML (2014) Inorg Chem 53:9460
74. Hanzelmann P, Dobbek H, Gremer L, Huber R, Meyer O (2000) J Mol Biol 301:1221
75. Dobbek H, Gremer L, Kiefersauer R, Huber R, Meyer O (2002) Proc Natl Acad Sci U S A 99:15971
76. Resch M, Dobbek H, Meyer O (2005) J Biol Inorg Chem 10:518
77. Stein BW, Kirk ML (2014) Chem Commun 50:1104
78. Hille R, Dingwall S, Wilcoxen J (2015) J Biol Inorg Chem 20:243
79. George GN, Pickering IJ, Yu EY, Prince RC, Bursakov SA, Gavel OY, Moura I, JJG M (2000) J Am Chem Soc 122:8321
80. Bursakov SA, Gavel OY, Di Rocco G, Lampreia J, Calvete J, Pereira AS, Moura JJ, Moura I (2004) J Inorg Biochem 98:833
81. Pauleta SR, Duarte AG, Carepo MS, Pereira AS, Tavares P, Moura I, Moura JJG (2007) Biomol NMR Assign 1:81
82. Rivas MG, Carepo MS, Mota CS, Korbas M, Durand MC, Lopes AT, Brondino CD, Pereira AS, George GN, Dolla A, Moura JJ, Moura I (2009) Biochemistry 48:873
83. Cvetkovic A, Menon AL, Thorgersen MP, Scott JW, Poole FL II, Jenney FE, Lancaster WA, Praissman JL, Shanmukh S, Vaccaro BJ, Trauger SA, Kalisiak E, Apon JV, Siuzdak G, Yannone SM, Tainer JA, Adams MWW (2010) Nature 466:779
84. Carepo MS, Pauleta SR, Wedd AG, Moura JJG, Moura I (2014) J Biol Inorg Chem 19:605
85. Enroth C, Eger BT, Okamoto K, Nishino T, Nishino T, Pai EF (2000) Proc Natl Acad Sci U S A 97:10723
86. Okamoto K, Matsumoto K, Hille R, Eger BT, Pai EF, Nishino T (2004) Proc Natl Acad Sci U S A 101:7931
87. Pauff JM, Zhang J, Bell CE, Hille R (2008) J Biol Chem 283:4818
88. Cao H, Hall J, Hille R (2014) Biochemistry 53:533
89. Stein BW, Kirk ML (2015) J Biol Inorg Chem 20:183
90. Massey V, Edmondson D (1970) J Biol Chem 245:6595
91. Malthouse JPG, Bray RC (1980) Biochem J 191:265
92. Mendel RR, Kruse T (2012) Biochem Biophys Acta 1823:1568
93. Mendel R (2013) J Biol Chem 288:13165
94. Mendel RR, Leimkuhler S (2015) J Biol Inorg Chem 20:337
95. Murray KN, Watson JG, Chaykin S (1966) J Biol Chem 241:4798
96. Hille R, Sprecher H (1987) J Biol Chem 262:10914

97. Xia M, Dempski R, Hille R (1999) J Biol Chem 274:3323
98. Stockert AL, Shinde S, Anderson RF, Hille R (2002) J Am Chem Soc 124:14554
99. Laughlin LJ, Young CG (1996) Inorg Chem 35:1050
100. Enemark JH, Cooney JJA, Wang J-J, Holm RH (2004) Chem Rev 104:1175
101. Sugimoto H, Tsukube H (2008) Chem Soc Rev 37:2609
102. Basu P, Burgmayer SJN (2015) J Biol Inorg Chem 20:373
103. Bray RC, Meriwether LS (1966) Nature 212:467
104. George GN, Bray RC (1988) Biochemistry 27:3603
105. Palmer G, Bray RC, Beinerrt H (1964) J Biol Chem 239:2657
106. Bray RC, Palmer G, Beinert H (1964) J Biol Chem 239:2667
107. Bray RC, Vanngard T (1969) Biochem J 114:725
108. Tanner S, Bray RC, Bergmann F (1978) Biochem Soc Trans 6:1328
109. Bray RC, George GN (1985) Biochem Soc Trans 13:560
110. Bray RC, Knowles PF, Meriwether LS (1967) ESR and the role of molybdenum in enzymic catalysis by xanthine oxidase. In: Ehrenberg A, Malmstrom BG, Vänngård T (eds) Magnetic resonance in biological systems. Pergamon Press, London
111. Edmondson DE, Ballou D, van Heuvelen A, Palmer G, Massey V (1973) J Biol Chem 248:6135
112. Hawkes TR, George GN, Bray RC (1984) Biochem J 218:961
113. McWhirter RB, Hille R (1991) J Biol Chem 266:23724
114. Gutteridge S, Bray RC (1980) Biochem J 189:615
115. Malthouse JPG, George GN, Lowe DJ, Bray RC (1981) Biochem J 197:421
116. Hanson GR, Wilson GL, Bailey TD, Pilbrow JR, Wedd AG (1987) J Am Chem Soc 109:2609
117. Massey V, Komai H, Palmer G, Elion GB (1970) J Biol Chem 246:2837
118. Drew SC, Hanson GR (2009) Inorg Chem 48:2224
119. Drew SC, Hill JP, Lane I, Hanson GR, Gable RW, Young CG (2007) Inorg Chem 46:2373
120. Drew SC, Young CG, Hanson GR (2007) Inorg Chem 46:2388
121. Bordas J, Bray RC, Garner CD, Gutteridge S, Hasnain S (1980) Biochem J 191:499
122. Malthouse JPG, George GN, Lowe DJ, Bray RC (1981) Biochem J 199:629
123. Wilson GL, Greenwood RJ, Pilbrow JR, Spence JT, Wedd AG (1991) J Am Chem Soc 113:6803
124. Cramer SP, Johnson JL, Rajagopalan KV, Sorrell TN (1979) Biochem Biophys Res Commun 91:434
125. Goodman BA, Raynor JB (1970) Adv Inorg Chem Radiochem 13:135
126. Hille R, Massey V (1985) Molybdenum-containing hydroxylases: xanthine oxidase aldehyde oxidase and sulfite oxidase. In: Spiro TG (ed) Molybdenum enzymes. Wiley, New York, NY, pp 443–518
127. Tullius TD, Kurtz DM Jr, Conradson SD, Hodgson KO (1979) J Am Chem Soc 101:2776
128. Howes BD, Bray RC, Richards RL, Turner NA, Bennett B, Lowe DJ (1996) Biochemistry 35:1432
129. Manikandan P, Choi E-Y, Hille R, Hoffman BM (2001) J Am Chem Soc 123:2658
130. Truglio JJ, Theis K, Leimkuhler S, Rappa R, Rajagopalan KV, Kisker C (2002) Structure 10:115
131. Gutteridge S, Tanner SJ, Bray RC (1978) Biochem J 175:869
132. Bray RC, Barber MJ, Lowe DJ (1978) Biochem J 171:653
133. Coughlan MP, Rajagopalan KV, Handler P (1969) J Biol Chem 244:2658
134. Pick FM, Bray RC (1969) Biochem J 114:735
135. Kanda M, Rajagopalan KV (1972) J Biol Chem 247:2177
136. Swann JC, Bray RC (1972) Eur J Biochem 26:407
137. Johnson JL, Waud WR, Cohen HJ, Rajagopalan KV (1974) J Biol Chem 249:5056
138. Gutteridge S, Tanner SJ, Bray RC (1978) Biochem J 175:887
139. Barber MJ, Coughlan MP, Kanda M, Rajagopalan KV (1980) Arch Biochem Biophys 201:468

140. Coughlan MP, Johnson JL, Rajagopalan KV (1980) J Biol Chem 255:2694
141. Maia L, Duarte RO, Ponces-Freire A, Moura JJG, Mira L (2007) J Biol Inorg Chem 12:777
142. Hille R, Kim JH, Hemann C (1993) Biochemistry 32:3973
143. Kim JH, Hille R (1993) J Biol Chem 268:44
144. Gutteridge S, Malthouse JPG, Bray RC (1979) J Inorg Biochem 11:355
145. Bray RC, Gutteridge S (1982) Biochemistry 21:5992
146. Morpeth FF, George GN, Bray RC (1984) Biochem J 220:235
147. Greenwood RJ, Wilson GL, Pilbrow JR, Wedd AG (1993) J Am Chem Soc 115:5385
148. Wilson GL, Kony M, Tiekink ERT, Pilbrow JR, Spence JT, Wedd AG (1988) J Am Chem Soc 110:6923
149. Bray RC, Knowles PF (1968) Proc R Soc Lond A 302:351
150. Malthouse JP, Bray RC (1983) Biochem J 215:101
151. Dowerah D, Spence JT, Singh R, Wedd AW, Wilson GL, Farchione F, Enemark JH, Kristofzski J, Bruckl M (1987) J Am Chem Soc 109:5655
152. Cammack R, Barber MJ, Bray RC (1976) Biochem J 157:469
153. Olson JS, Ballou DP, Palmer G, Massey V (1974) J Biol Chem 249:4363
154. Palmer G, Massey V (1969) J Biol Chem 244:2614
155. Barber MJ, Bray RC, Cammack R, Coughlan MP (1977) Biochem J 163:279
156. Bray RC, Knowles PF, Pick FM, Vänngård T (1968) Biochem J 107:601
157. Edmondson D, Massey V, Palmer G, Beacham LM, Elion GB (1972) J Biol Chem 247:1597
158. Pick FM, McGartoll MA, Bray RC (1971) Eur J Biochem 18:65
159. Howes BD, Pinhal NM, Turner NA, Bray RC, Anger G, Ehrenberg A, Raynor JB, Lowe DJ (1990) Biochemistry 29:6120
160. Shanmugam M, Zhang B, McNaughton RL, Kinney RA, Hille R, Hoffman BM (2010) J Am Chem Soc 132:14015
161. Lowe DJ, Barber MJ, Pawlik RT, Bray RC (1976) Biochem J 155:81
162. Hille R, Stewart RC, Fee JA, Massey V (1983) J Biol Chem 258:4849
163. Stewart RC, Hille R, Massey V (1984) J Biol Chem 259:14426
164. Barber MJ, Siegel LM (1983) Biochemistry 22:618
165. George GN, Bray RC (1983) Biochemistry 22:1013
166. Cramer SP, Hille R (1985) J Am Chem Soc 107:8164
167. Cao H, Hall J, Hille R (2011) J Am Chem Soc 133:12414
168. George GN, Bray RC (1983) Biochemistry 22:5443
169. Hille R, Hagen WR, Dunham WR (1985) J Biol Chem 260:10569
170. Lowe DJ, Lynden-Bell RM, Bray RC (1972) Biochem J 130:239
171. Lowe DJ, Bray RC (1978) Biochem J 169:471
172. Canne C, Lowe DJ, Fetzner S, Adams B, Smith AT, Kappl R, Bray RC, Hüttermann J (1999) Biochemistry 38:14077
173. Caldeira J, Belle V, Asso M, Guigliarelli B, Moura I, Moura JJG, Bertrand P (2000) Biochemistry 39:2700
174. More C, Asso M, Roger G, Guigliarelli B, Caldeira J, Moura J, Bertrand P (2005) Biochemistry 44:11628
175. Rupp H, Rao KK, Hall DO, Cammack R (1978) Biochim Biophys Acta 537:255
176. Barber MJ, Salerno JC, Siegel LM (1982) Biochemistry 21:1648
177. Coffman RE, Buettner GR (1979) J Phys Chem 83:2392
178. Moura JJG, Xavier AV, Bruschi M, Le Gall J, Hall DO, Cammack R (1976) Biochem Biophys Res Commun 72:782
179. Turner N, Barata B, Bray RC, Deistung J, Le Gall J, Moura JJ (1987) Biochem J 243:755
180. Barata BA, LeGall J, Moura JJ (1993) Biochemistry 32:11559
181. Romão MJ, Archer M, Moura I, Moura JJG, LeGall J, Engh R, Schneider M, Hof P, Huber R (1995) Science 270:1170
182. Huber R, Hof P, Duarte RO, Moura JJG, Moura I, Liu M-Y, Legall J, Hille R, Archer M, Romão MJ (1996) Proc Natl Acad Sci USA 93:8846

183. Rebelo JM, Dias JM, Huber R, Moura JJG, Romão MJ (2001) J Biol Inorg Chem 6:791
184. Krippahl L, Palma N, Moura I, Moura JJG (2006) Eur J Inorg Chem 19:3835
185. Barata BA, Liang J, Moura I, LeGall J, Moura JJG, Huynh BH (1992) Eur J Biochem 204:773
186. Duarte RO, Archer M, Dias JM, Bursakov S, Huber R, Moura I, Romão MJ, Moura JJG (2000) Biochem Biophys Res Commun 268:745
187. Santos-Silva T, Ferroni F, Thapper A, Marangon J, Gonzalez PJ, Rizzi AC, Moura I, Moura JJG, Romão MJ, Brondino CD (2009) J Am Chem Soc 131:7990
188. Mehra RK, Coughlan MP (1984) Arch Biochem Biophys 229:585
189. Coughlan MP, Mehra RK, Barber MJ, Siegel LM (1984) Arch Biochem Biophys 229:596
190. Boer DR, Thapper A, Brondino CD, Romão MJ, Moura JJG (2004) J Am Chem Soc 126:8614
191. Thapper A, Boer DR, Brondino CD, Moura JJG, Romao MJ (2007) J Biol Inorg Chem 12:353–366
192. Gladyshev VN, Khangulov SV, Stadtman TC (1994) Proc Natl Acad Sci USA 91:232
193. Schrader T, Rienhofer A, Andreesen JR (1999) Eur J Biochem 264:862
194. Self WT, Stadtman TC (2000) Proc Natl Acad Sci USA 97:7208
195. Wagener N, Pierik AJ, Ibdah A, Hille R, Dobbek H (2009) Proc Natl Acad Sci USA 106:11055
196. Hofmann M, Kassube JK, Graf T (2005) J Biol Inorg Chem 10:490
197. Siegbahn PEM, Shestakov AF (2005) J Comput Chem 26:888
198. Zhang B, Hemann CF, Hille R (2010) J Biol Chem 285:12571
199. Gourlay C, Nielsen DJ, White JM, Knottenbelt SZ, Kirk ML, Young CG (2006) J Am Chem Soc 128:2164
200. Wilcoxen J, Snider S, Hille R (2011) J Am Chem Soc 133:12934
201. Gnida M, Ferner R, Gremer L, Meyer O, Meyer-Klaucke W (2003) Biochemistry 42:222
202. Shanmugam M, Wilcoxen J, Habel-Rodriguez D, Cutsail GEI, Kirk ML, Hoffman BM, Hille R (2013) J Am Chem Soc 135:17775
203. Feng C, Tollin G, Enemark JH (2007) Biochim Biophys Acta 1774:527
204. Kappler U, Enemark JH (2015) J Biol Inorg Chem 20:253
205. Loschi L, Brokx SJ, Hills TL, Zhang G, Bertero MG, Lovering AL, Weiner JH, Strynadka NCJ (2004) J Biol Chem 279:50391
206. George GN, Doonan CJ, Rothery RA, Boroumand N, Weiner JH (2007) Inorg Chem 46:2
207. Havelius KGV, Reschke S, Horn S, Doerlng A, Niks D, Hille R, Schulzke C, Leimkuehler S, Haumann M (2011) Inorg Chem 50:741
208. Ott G, Havemeyer A, Clement B (2015) J Biol Inorg Chem 20:265
209. Kisker C, Schindelin H, Pacheco A, Wehbi WA, Garrett RM, Rajagopalan KV, Enemark JH, Rees DC (1997) Cell 91:973
210. Griffith OW (1987) Methods Enzymol 143:366
211. Pacheco A, Hazzard JT, Tollin G, Enemark JH (1999) J Biol Inorg Chem 4:390
212. Feng CJ, Kedia RV, Hazzard JT, Hurley JK, Tollin G, Enemark JH (2002) Biochemistry 41:5816
213. Johnson-Winters K, Nordstrom AR, Emesh S, Astashkin AV, Rajapakshe A, Berry RE, Tollin G, Enemark JH (2010) Biochemistry 49:1290
214. Hille R (1994) Biochim Biophys Acta 1184:143
215. Brody MS, Hille R (1995) Biochim Biophys Acta 1253:133
216. Pietsch MA, Hall MB (1996) Inorg Chem 35:1273
217. Brody MS, Hille R (1999) Biochemistry 38:6668
218. Thomson LM, Hall MB (2001) J Am Chem Soc 123:3995
219. Peariso K, McNaughton RL, Kirk ML (2002) J Am Chem Soc 124:9006
220. Wilson HL, Rajagopalan KV (2004) J Biol Chem 279:15105
221. Kail BW, Perez LM, Zaric SD, Millar AJ, Young CG, Hall MB, Basu P (2006) Chem Eur J 12:7501
222. Bailey S, Rapson T, Winters-Johnson K, Astashkin AV, Enemark JH, Kappler U (2009) J Biol Chem 284:2053
223. Byrne RS, Haensch R, Mendel RR, Hille R (2009) J Biol Chem 284:35479

224. Cohen HJ, Fridovich I, Rajagopalan KV (1971) J Biol Chem 246:374
225. Kessler DL, Rajagopalan KV (1972) J Biol Chem 247:6566
226. Kessler DL, Johnson JL, Cohen HJ, Rajagopalan KV (1974) Biochim Biophys Acta 334:86
227. Kessler DL, Rajagopalan KV (1974) Biochim Biophys Acta 370:389
228. Johnson JL, Rajagopalan KV (1976) J Biol Chem 251:5505
229. Gutteridge S, Lamy MT, Bray RC (1980) Biochem J 191:285
230. Lamy MT, Gutteridge S, Bary RC (1980) Biochem J 185:397
231. Bray RC, Lamy MT, Gutteridge S, Wilkinson T (1982) Biochem J 201:241
232. Astashkin AV, Raitsimring AM, Feng CJ, Johnson JL, Rajagopalan KV, Enemark JH (2002) J Am Chem Soc 124:6109
233. Garton SD, Garrett RM, Rajagopalan KV, Johnson MK (1997) J Am Chem Soc 119:2590
234. Astashkin AV, Johnson-Winters K, Klein EL, Feng C, Wilson HL, Rajagopalan KV, Raitsimring AM, Enemark JH (2008) J Am Chem Soc 130:8471
235. Enemark JH, Raitsimring AM, Astashkin AV, Klein EL (2011) Faraday Discuss 148:249
236. Klein EL, Raitsimring AM, Astashkin AV, Rajapakshe A, Johnson-Winters K, Arnold AR, Potapov A, Goldfarb D, Enemark JH (2012) Inorg Chem 51:1408
237. Bray RC, Gutteridge S, Lamy MT, Wilkinson T (1983) Biochem J 211:227
238. Astashkin AV, Klein EL, Enemark JH (2007) J Inorg Biochem 101:1623
239. Doonan CJ, Wilson HL, Bennett B, Prince RC, Rajagopalan KV, George GN (2008) Inorg Chem 47:2033
240. Klein EL, Astashkin AV, Ganyushin D, Riplinger C, Johnson-Winters K, Neese F, Enemark JH (2009) Inorg Chem 48:4743
241. Karakas E, Wilson HL, Graf TN, Xiang S, Jaramillo-Buswuets S, Rajagopalan KV, Kisker C (2005) J Biol Chem 280:33506
242. Pushie MJ, Doonan CJ, Wison HL, Rajagopalan KV, George GN (2011) Inorg Chem 50:9406
243. Rajapakshe A, Johnson-Winters K, Nordstrom AR, Meyers KT, Emesh S, Astashkin AV, Enemark JH (2010) Biochemistry 49:5154
244. Astashkin AV, Johnson-Winters K, Klein EL, Byrne RS, Hille R, Raitsimring AM, Enemark JH (2007) J Am Chem Soc 129:14800
245. Astashkin AV, Hood BL, Feng C, Hille R, Mendel RR, Raitsimring AM, Enemark JH (2005) Biochemistry 44:13274
246. Doonan CJ, Wilson HL, Garrett RM, Bennet B, Prince RC, Rajagopalan KV, George GM (2007) J Am Chem Soc 129:9421
247. Garrett RM, Rajagopalan KV (1996) J Biol Chem 271:7387
248. George GN, Garrett RM, Prince RC, Rajagopalan KV (1996) J Am Chem Soc 118:8588
249. Qiu JA, Wilson HL, Pushie MJ, Kisker C, George GN, Rajagopalan KV (2010) Biochemistry 49:3989
250. George GN, Garrett RM, Prince RC, Rajagopalan KV (2004) Inorg Chem 43:8456
251. Reschke S, Niks D, Wilson H, Sigfridsson KGV, Haumann M, Rajagopalan KV, Hille R, Leimkuhler S (2013) Biochemistry 52:8295
252. Raitsimring AM, Pacheco A, Enemark JH (1998) J Am Chem Soc 120:11263
253. Astashkin AV, Mader ML, Pacheco A, Enemark JH, Raitsimring AM (2000) J Am Chem Soc 122:5294
254. George GN (1985) J Magn Reson 64:384
255. Astashkin AV, Feng CJ, Raitsimring AM, Enemark JH (2005) J Am Chem Soc 127:502
256. Astashkin AV, Neese F, Raitsimring AM, Cooney JJA, Bultman E, Enemark JH (2005) J Am Chem Soc 127:16713
257. Peariso K, Chohan BS, Carrano CJ, Kirk ML (2003) Inorg Chem 42:6194
258. George GN, Prince RC, Kipke CA, Sunde RA, Enemark JH (1988) Biochem J 256:307
259. Pacheco A, Basu P, Borbat P, Raitsimring AM, Enemark JH (1996) Inorg Chem 35:7001
260. George GN, Garrett RM, Graf T, Prince RC, Rajagopalan KV (1998) J Am Chem Soc 120:4522
261. Schink B (1985) Arch Microbiol 142:295

262. Messerschmidt A, Niessen H, Abt D, Einsle O, Schink B, Kroneck PM (2004) Proc Natl Acad Sci U S A 101:11571
263. Moura JJ, Brondino CD, Trincao J, Romao MJ (2004) J Biol Inorg Chem 9:791
264. Jormakka M, Yokoyama K, Yano T, Tamakoshi M, Akimoto S, Shimamura T, Curmi P, Iwata S (2008) Nat Struct Mol Biol 15:730
265. Rothery RA, Workun GJ, Weiner JH (2008) Biochim Biophys Acta 1778:1897
266. Ellis PJ, Conrads T, Hille R, Kuhn P (2001) Structure 9:125
267. Conrads T, Hemann C, George GN, Pickering IJ, Prince RC, Hille R (2002) J Am Chem Soc 124:11276
268. Silver S, Phung LT (2005) Appl Environ Microbiol 71:599
269. Warelow TP, Oke M, Schoepp-Cothenet B, Dahl JU, Bruselat N, Sivalingam GN, Leimkuhler S, Thalassinos K, Kappler U, Naismith JH, Santini JM (2013) PLoS One 8:e72535
270. Potter L, Angove H, Richardson D, Cole J (2001) Adv Microb Physiol 45:51
271. Stolz JF, Basu P (2002) ChemBioChem 3:198
272. Bertero MG, Rothery RA, Palak M, Hou C, Lim D, Blasco F, Weiner JH, Strynadka NCJ (2003) Nat Struct Biol 10:681
273. Jormakka M, Richardson D, Byrne B, Iwata S (2004) Structure 12:95
274. González PG, Correia C, Moura I, Brondino CD, Moura JJG (2006) J Inorg Biochem 100:1015
275. Martinez-Espinosa RM, Dridge EJ, Bonete MJ, Butt JN, Butler CS, Sargent F, Richardson DJ (2007) FEMS Microbiol Lett 276:129
276. Kraft B, Strous M, Tegetmeyer HE (2011) J Biotechnol 155:104
277. Gonzalez PJ, Mota CS, Brondino CD, Moura I, Moura JJG (2013) Coord Chem Rev 257:315
278. Sparacino-Watkins C, Stolzb JF, Basu P (2014) Chem Soc Rev 43:676
279. Bertero MG, Rothery RA, Boroumand N, Palak M, Blasco F, Ginet N, Weiner JH, Strynadka NCJ (2005) J Biol Chem 280:14836
280. Dias JM, Than ME, Humm A, Huber R, Bourenkov GP, Bartunik HD, Bursakov S, Calvete J, Caldeira J, Carneiro C, Moura JJG, Moura I, Romão MJ (1999) Structure 7:65
281. Najmudin S, Gonzalez PJ, Trincao J, Coelho C, Mukhopadhyay A, Cerqueira N, Romão CC, Moura I, Moura JJG, Brondino CD, Romão MJ (2008) J Biol Inorg Chem 13:773
282. Coelho C, Gonzalez PJ, Moura JJG, Moura I, Trincao J, Romão MJ (2011) J Mol Biol 408:932
283. Coelho C, Gonzalez PJ, Trincão J, Carvalho AL, Najmudin S, Hettman T, Dieckman S, Moura JJG, Moura I, Romão MJ (2007) Acta Crystallogr F 63:516
284. Jepson BJN, Mohan S, Clarke TA, Gates AJ, Cole JA, Butler CS, Butt JN, Hemmings AM, Richardson DJ (2007) J Biol Chem 282:6425
285. Arnoux P, Sabaty M, Alric J, Frangioni B, Guigliarelli B, Adriano JM, Pignol D (2003) Nat Struct Biol 10:928
286. Jepson BJN, Anderson LJ, Rubio LM, Taylor CJ, Butler CS, Flores E, Herrero A, Butt JN, Richardson DJ (2004) J Biol Chem 279:32212
287. Trchounian K, Poladyan A, Vassilian A, Trchounian A (2012) Crit Rev Biochem Mol Biol 47:236
288. Bagramyan K, Trchounian A (2003) Biochem Mosc 68:1159
289. Jones RW, Lamont A, Garland PB (1980) Biochem J 190:79
290. Berg BL, Li J, Heider J, Stewart V (1991) J Biol Chem 266:22380
291. Blasco F, Guigliarelli B, Magalon A, Asso M, Giordano G, Rothery RA (2001) Cell Mol Life Sci 58:179
292. Jormakka M, Tornroth S, Byrne B, Iwata S (2002) Science 295:1863
293. Richardson D, Sawers G (2002) Science 295:1842
294. Jormakka M, Byrne B, Iwata S (2003) Curr Opin Struct Biol 13:418
295. Jormakka M, Byrne B, Iwata S (2003) FEBS Lett 545:25
296. Sawers G, Heider J, Zehelein E, Bock A (1991) J Bacteriol 173:4983
297. Pommier J, Mandrand MA, Holt SE, Boxer DH, Giodano G (1992) Biochim Biophys Acta 1107:305

298. Sawers G (1994) Antonie Van Leeuwenhoek 66:57
299. Abaibou H, Pommier J, Benoit S, Giordano G, Mandrandberthelot MA (1995) J Bacteriol 177:7141
300. Benoit S, Abaibou H, Mandrand-Berthelot MA (1998) J Bacteriol 180:6625
301. Friedebold J, Bowien B (1993) J Bacteriol 175:4719
302. Friedebold J, Mayer F, Bill E, Trautwein AX, Bowien B (1995) Biol Chem Hoppe Seyler 376:561
303. Boyington JC, Gladyshev VN, Khangulov SV, Stadtman TC, Sun PD (1997) Science 275:1305
304. Costa C, Teixeira M, LeGall J, Moura JJG, Moura I (1997) J Biol Inorg Chem 2:198
305. Oh JI, Bowien B (1998) J Biol Chem 273:26349
306. Raaijmakers HCA, Romão MJ (2006) J Biol Inorg Chem 11:849
307. Rivas M, Gonzalez P, Brondino CD, Moura JJG, Moura I (2007) J Inorg Biochem 101:1617
308. Thome R, Gust A, Toci R, Mendel R, Bittner F, Magalon A, Walburger A (2012) J Biol Chem 287:4671
309. Hartmann T, Leimkuhler S (2013) FEBS J 280:6083
310. Gladyshev VN, Khangulov SV, Axley MJ, Stadtman TC (1994) Proc Natl Acad Sci U S A 91:7708
311. Gladyshev VN, Boyington JC, Khangulov SV, Grahame DA, Stadtman TC, Sun PD (1996) J Biol Chem 271:8095
312. Khangulov SV, Gladyshev VN, Dismukes GC, Stadtman TC (1998) Biochemistry 37:3518
313. George GN, Colangelo CM, Dong J, Scott RA, Khangulov SV, Gladyshev VN, Stadtman TC (1998) J Am Chem Soc 120:1267
314. Niks D, Duvvuru J, Escalona M, Hille R (2016) J Biol Chem 291:1162
315. Maia LB, Fonseca L, Moura I, Moura JJG (2016) J Am Chem Soc 138:8834
316. Raaijmakers H, Macieira S, Dias JM, Teixeira S, Bursakov S, Huber R, Moura JJG, Moura I, Romão MJ (2002) Structure 10:1261
317. George GN, Costa C, Moura JJG, Moura I (1999) J Am Chem Soc 121:2625
318. Jollie DR, Lipscomb JD (1991) J Biol Chem 266:21853
319. Brondino CD, Passeggi MCG, Caldeira J, Almendra MJ, Feio MJ, Moura JJG, Moura I (2004) J Biol Inorg Chem 9:145
320. Hagedoorn PL, Hagen WR, Stewart LJ, Docrat A, Bailey S, Garner CD (2003) FEBS Lett 555:606
321. Gonzalez PJ, Rivas MG, Brondino CD, Bursakov SA, Moura I, Moura JJG (2006) J Biol Inorg Chem 11:609
322. Najmudin S, Gonzalez PJ, Trincao J, Coelho C, Mukhopadhyay A, Cerqueira N, Romão CC, Moura I, Moura JJG, Brondino CD, Romão MJ (2008) J Biol Inorg Chem 13:737
323. Bennett B, Berks BC, Ferguson SJ, Thomson AJ, Richardson DJ (1994) Eur J Biochem 226:789
324. Butler CS, Charnock JM, Bennett B, Sears HJ, Reilly AJ, Ferguson SJ, Garner CD, Lowe DJ, Thomson AJ, Berks BC, Richardson DJ (1999) Biochemistry 38:9000
325. Butler CS, Charnock JM, Garner CD, Thomson AJ, Ferguson SJ, Berks BC, Richardson DJ (2000) Biochem J 352:859
326. Butler CS, Fairhurst SA, Ferguson SJ, Thomson AJ, Berks BC, Richardson DJ, Lowe DJ (2002) Biochem J 363:817
327. Bertrand P, Frangioni B, Dementin S, Sabaty M, Arnoux P, Guigliarelli B, Pignol D, Leger C (2007) J Phys Chem B 111:10300
328. Fourmond V, Burlat B, Dementin S, Arnoux P, Sabaty M, Boiry S, Guigliarelli B, Bertrand P, Pignol D, Leger C (2008) J Phys Chem B 112:15478
329. Simpson PJL, McKinzie AA, Codd R (2010) Biochem Biophys Res Commun 398:13
330. Simpson PJL, Richardson DJ, Codd R (2010) Microbiology 156:302
331. Biaso F, Burlat B, Guigliarelli B (2012) Inorg Chem 51:3409
332. Nemykin VN, Basu P (2003) Inorg Chem 42:4046

333. Gangeswaran R, Lowe DJ, Eady RR (1993) Biochem J 289:335
334. Bray RC, Vincent SP, Lowe DJ, Clegg RA, Garland PB (1976) Biochem J 155:201
335. Clegg RA (1976) Biochem J 153:533
336. Vincent SP, Bray RC (1978) Biochem J 171:639
337. Godfrey C, Greenwood C, Thomson AJ, Bray RC, George GN (1984) Biochem J 224:601
338. George GN, Bray RC, Morpeth FF, Boxer DH (1985) Biochem J 227:925
339. Turner N, Ballard AL, Bray RC, Ferguson SJ (1988) Biochem J 252:925
340. Magalon A, Asso M, Guigliarelli B, Rothery RA, Bertrand P, Giordano G, Blasco F (1998) Biochemistry 37:7363
341. Hettmann T, Anemuller S, Borcherding H, Mathe L, Steinrucke P, Diekmann S (2003) FEBS Lett 534:143
342. Correia C, Besson S, Brondino CD, Gonzalez PJ, Fauque G, Lampreia J, Moura I, Moura JJG (2008) J Biol Inorg Chem 13:1321
343. Field SJ, Thornton NP, Anderson LJ, Gates AJ, Reilly A, Jepson BJN, Richardson DJ, George SJ, Cheesman MR, Butt JN (2005) Dalton Trans:3580
344. Anderson LJ, Richardson DJ, Butt JN (2001) Biochemistry 40:11294
345. Anderson LJ, Richardson DJ, Butt JN (2000) Faraday Discuss 116:155
346. George GN, Turner NA, Bray RC, Morpeth FF, Boxer DH, Cramer SP (1989) Biochem J 259:693